Final Report: Analysis of Silicon Photonics Mach-Zehnder Interferometers

Dr Piyush Kumar (edX: drpkoffice)

GDS File: EBeam_DRPKOFFICE.gds

Abstract

This report presents the learning outcomes of the edX course on Silicon Photonics Design, Fabrication and Data Analysis, which itself is based on these works [1–3]. The objective of this report is to outline the designing of Mach-Zehnder interferometers (MZIs) which are then simulated, fabricated, and tested to compare the MZIs with each other and to compare the experimental data with the simulation data. The MZIs differ from each other in their path length differences (ΔL) and the resulting transmission or insertion loss are analyzed to obtain and study the impact of ΔL on the free spectral range (FSR) and group index of the MZIs. There are 7 MZIs and 2 reference devices (2 grating couplers connected by a single waveguide) tested in this report. Due to variations and imperfections in manufacturing, optical loss into materials, coupling loss, and environmental effects, the insertion loss is higher in the measured dataset than in the simulated MZI dataset. The measured FSR and group index values of all the MZIs have been found to fall within <1% of the their simulated FSR and group index counterparts in the majority of the data points. This also shows a high degree of manufacturing precision and that other than the higher optical loss in real world, there are no other significant differences between the theoretical and applied aspects of silicon photonic circuitry.

1. Introduction

A Mach-Zehnder Interferometer (MZI) is an optical device which introduces differences in optical path lengths of two light beams and then measure phase shifts in light. It is used as an important tool in physics and engineering for studying phase shifts, interference (constructive, destructive, partial), detecting small changes in refractive index, and nowadays even in quantum mechanics experiments. In macroscopic applications, an MZI consists of a light source and a series of beam splitters and reflective mirrors. In the field of silicon photonics, it consists of (in addition to a light source) grating couplers, directional couplers, waveguides, and Y-branch splitters. It can also include additional components such as thermal heaters to induce phase shifts through refractive index shifts, which also help in fine-tuning the performance of fabricated MZIs.

In this project, 7 passive and imbalanced MZIs are designed, fabricated and tested to obtain the MZI transfer function over the wavelength range of 1500 to 1600 nm and then calculate the free spectral range (FSR) of the MZI and the silicon waveguide's group index, effective index and group velocity of the light travelling in the fabricated silicon waveguide. They are simple MZIs and the only variable parameter is the path length difference between the two waveguides as shown in Table 2 in Section 3. Six MZIs have one waveguide kept constant at 150 µm in length, while the other waveguide is of different lengths in different MZIs to obtain different path length differences (ΔL) of 25, 50, 100, 150, 200, and 400 µm. One out of the seven MZIs also includes a broadband directional coupler (50-50 splitter) and has a waveguide path length difference of 180 µm. In addition, there are also two reference devices, each containing one waveguide of length 150 µm and 300 µm connected with a grating coupler at both the ends. Thus, there are a total of 9 photonic circuits designed to be fabricated.

The waveguides are of the strip-waveguide type with the dimensions of 500 nm in width and 220 nm in height. The grating couplers (GCs) are of quasi-TE type and the distance between the input and output GCs is kept constant precisely at 127 µm to align with the commercial measuring optic fibre fiber array. The splitter and combiner are Y-branch type for 50-50 beam splitting.

2. Theory

2.1 Mach-Zehnder Interferometer (MZI): In an MZI, light is coupled from an external source to a photonic circuit through a grating coupler and it is then split into two equal beams with a Y-branch splitter. The two beams then travel through the two waveguides of unequal lengths and, as a result, undergo phase shift with respect to each other. The phase-shifted lights then combine through a Y-branch combiner into one waveguide and then outputted through the output grating coupler. Depending on the phase shift, the lights interfere constructively or destructively or obtain a value in-between. If an ideal 50-50% beam splitter is used, then mathematically, the output light intensity (Io) in each of the two waveguides is half of the input light intensity (Ii) (eq. 2) and the output electric field value (Eo) is equal to the input electric field (Ei) value divided by square-root of 2 (eq. 3), which is because light intensity or power is directly proportional to the square of the electric field (eq. 1).

$$\mathrm{I_i} \propto |\mathrm{E}|^2 \qquad \text{(eq. 1)}$$

$$\mathrm{Io} = \frac{\mathrm{Ii}}{2} \qquad \text{(eq. 2)}$$

$$\mathrm{Eo} = \frac{\mathrm{Ei}}{\sqrt{2}} \qquad \text{(eq. 3)}$$

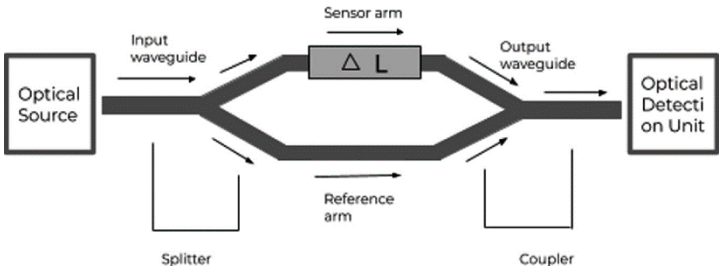

Figure 1: Schematic illustration of a Mach Zehnder Interferometer [4].

2.2 Effective Index (neff): The effective index of a waveguide is an equivalent of refractive index that a guided light mode experiences and is dependent not only on the material, wavelength, and temperature, etc. but also on the dimensions of the structure (waveguide). In other words, it describes how the light wave physically propagates as a combined function of a waveguide's material and its geometric dimensions. The effective index as a function of the wavelength can be expressed as a second-order Taylor expansion or a quadratic fit or a polynomial expression as shown by the equation below (eq. 4). This equation helps in

correctly calculating a waveguide's effective index at different wavelengths provided the other parameters, such as material, dimensions, temperature, etc., remain constant. Hence, this equation is also called as the compact model of a waveguide.

$$n_{eff}(\lambda) = n_1 + n_2(\lambda - \lambda_0) + n_3(\lambda - \lambda_0)^2 \quad \text{(eq. 4)}$$

Here, n1 is a zeroth order term and is the known effective index at a reference or central wavelength, such as 1550 nm (λ_0), of a given range of wavelengths tested; n2 is the first order dispersion coefficient or the slope of the effective index curve obtained when a wavelength or frequency sweep is done on either side of the central wavelength and it shows how fast the effective index changes on changing wavelength; and n3 is the second order dispersion coefficient or curvature or the rate-of-change of change-in-effective-index over a range of wavelengths centered around a central wavelength (if n3 is 0 then it means a perfectly linear slope, which is an ideal situation, not observed in real world).

2.3 Group Index (ng): The group index of a waveguide describes how the effective index changes with wavelength or how a group of wavelengths travelling together disperses collectively within a structure such as a waveguide. The following equations show the relation between group index and effective index (eq. 5 and eq. 6).

$$\text{Group index, } n_g = n_{eff} - \lambda \frac{dn_{eff}}{d\lambda} \quad \text{(eq. 5)}$$

Since, $n_2 = \frac{dn_{eff}}{d\lambda}$, the eq. 5 can be rewritten as,

$$\text{Group index, } n_g = n_1 - \lambda_0 n_2 \quad \text{(eq. 6)}$$

2.4 Group Velocity (vg): The group velocity is the speed at which a pulse of light consisting of multiple wavelengths propagate through a structure, such as a waveguide, and is dependent on the waveguide's material, dimensions, and dispersion characteristics. It can be obtained by dividing the speed of light in vacuum (c) by the effective index (neff) of the waveguide (eq. 7). Two related concepts are dispersion parameter and group velocity dispersion. The dispersion parameter (D) describes how a light pulse broadens per unit wavelength and distance as it propagates through a waveguide or optic fiber and is given by the below mentioned equation (eq. 8). The group velocity dispersion (GVD) describes how different parts or wavelengths of a light pulse in a waveguide travel at slightly different velocities with respect to each other and is given by the following equations (eq. 7 and eq. 9).

$$v_g = \frac{c}{n_{eff}} \quad \text{(eq. 7)}$$

$$GVD = -\frac{\lambda^2}{2\pi c} D \quad \text{(eq. 8)}$$

$$\text{and, } D = -\frac{\lambda}{c} \frac{d^2 n_{eff}}{d\lambda^2} \quad \text{(eq. 9)}$$

$$\text{Thus, } GVD = \frac{\lambda^3}{2\pi c^2} \frac{d^2 n_{eff}}{d\lambda^2} \quad \text{(eq. 10)}$$

3. Modelling and Simulation

For modelling and simulating the photonic components and circuits, Ansys Lumerical MODE is used for silicon waveguides and Ansys Lumerical INTERCONNECT is used for the MZIs.

3.1 Waveguide Simulation: In MODE, the eigenmode analysis is done by laying out the geometry of photonic components (waveguide here), applying parameters such as dimensions of the waveguide and wavelength of light, meshing of the waveguide, and then calculating the mode which then generates the effective indices for different mode values.

Table 1: Parameters used in Waveguide modelling in MODE.

Core	Silicon (Si)
Cladding	Silicon Dioxide (SiO_2)
Type	Strip
Height	220 nm
Width	500 nm
Bend Radius	No bend, 5 µm bend
Wavelength	1550 nm, 1500-1600 nm
Polarization	TE or quasi-TE

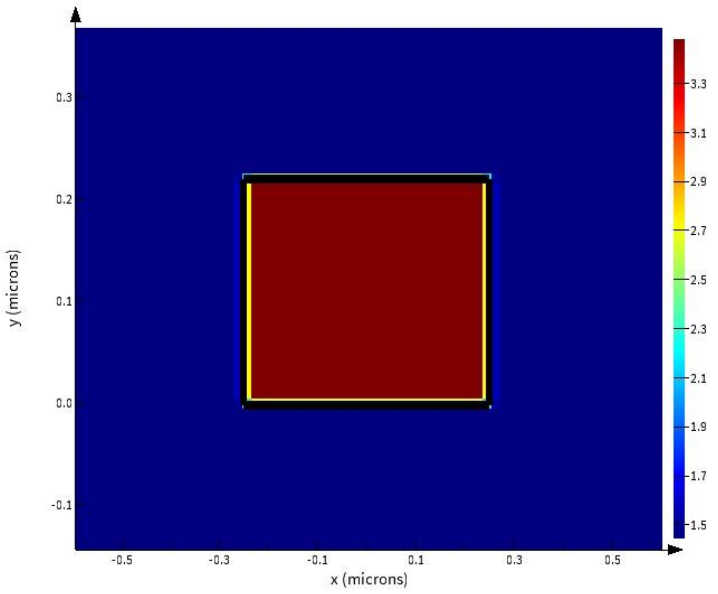

Figure 2: Cross section of a meshed silicon waveguide with dimensions of 220nm by 500nm as observed in Ansys MODE.

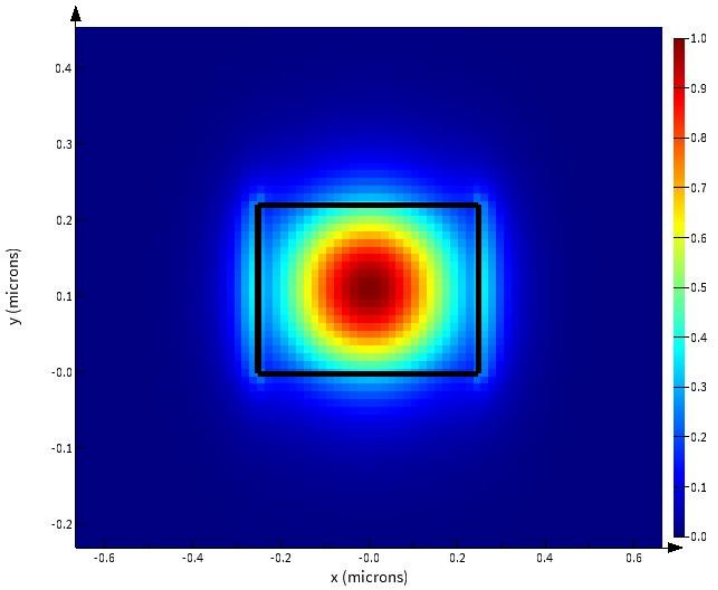

Figure 3: Simulated modes in the modelled waveguide (220nm x 500nm) as observed in Ansys MODE.

On applying the parameters laid out in table 1, the eigenmode solving gives the effective index at 1550 nm to be 2.4468 for TE or quasi-TE polarization. The group index is approximately 4.2.

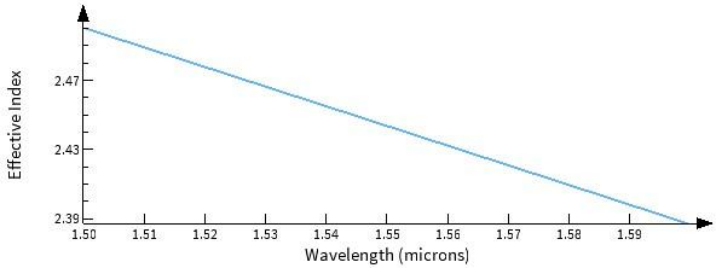

Figure 4: Wavelength or frequency sweep graph showing change in effective index of a 220 x 500 nm strip waveguide as a function of wavelength from 1500 nm to 1600 nm.

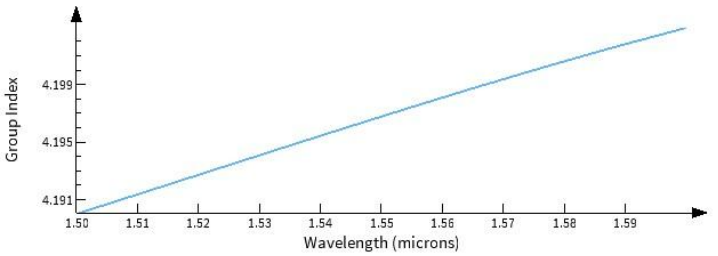

Figure 5: Wavelength or frequency sweep graph showing change in group index of a 220 x 500 nm strip waveguide as a function of wavelength from 1500 to 1600 nm.

From figures 5 and 6 above, it can be deduced that the effective index (neff) decreases with increasing wavelength, whereas the group index (ng) increases with increasing wavelength.

The equation 4 above can be centered, for example, at $\lambda 0$ = 1.55 as shown by the equation below. The values of n1, n2 and n3 can be obtained from the eigenmode solving simulation after frequency sweeping in Ansys MODE. The effective index for this particular simulated waveguide at a given wavelength λ thus becomes:

$$n_{eff} = [2.44 - 1.13 * (\lambda - 1.55)] - [0.04 * (\lambda - 1.55)^2]$$

Additionally, by adding a bend in the waveguide and then eigenmode solving shows a differential loss between the outer and inner side walls of a waveguide, with outer side wall showing greater optical loss as shown in the figure 6 below.

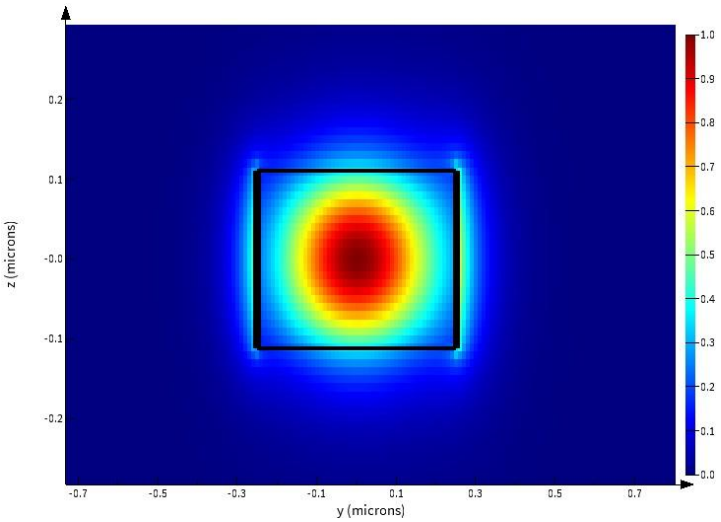

Figure 6: Simulated modes in a bent waveguide (220nm x 500nm; bend radius = 5µm). The simulation shows differential loss on the two sides owing to the bend, with greater loss towards the right side which is the outer edge of the waveguide.

3.2 MZI Simulation (Model): In INTERCONNECT, an MZI is laid out with constant parameters and several simulations are run with only one variable parameter which is the path length difference (ΔL) between the two waveguides. The structure consists of an input and an output grating couplers connected respectively to a Y-branch splitter and a Y-branch combiner which are themselves connected to each other by two identical waveguides with a known path length difference between them. The schematic of such an MZI is shown in the figure below.

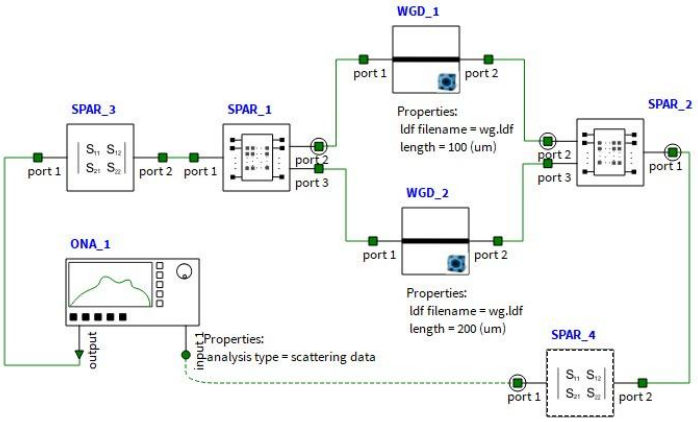

Figure 7: Layout of an example MZI in Ansys INTERCONNECT as observed in the Root Element layout.

3.3 MZI Simulation (Transfer Function): In silicon photonics, propagation constant (β) of light means the rate of change of phase as it travels through the waveguide. It is calculated as follows:

$$\beta = \frac{2\pi n_{eff}}{\lambda} \qquad \text{(eq. 10)}$$

Transfer function of a Mach-Zehnder Interferometer describes how an input light gets modified before exiting an MZI as output light. It is calculated as output light intensity as a function of the input light intensity and the phase difference

between the two waveguides of the MZI. It is mathematically expressed as:

$$\frac{I_o}{I_i}\,(\mathrm{MZI}) = \frac{1}{2}\,[1 + \cos(\beta \Delta L)] \qquad \text{(eq. 11)}$$

Here, Ii is input light intensity, β is propagation constant of light and ΔL is the path length difference between the two waveguides of the MZI.

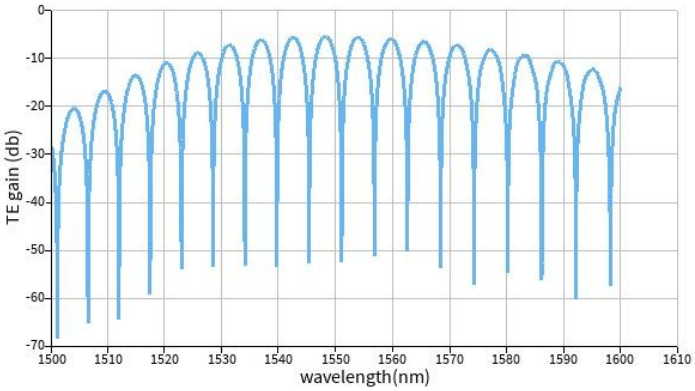

Figure 8: Transfer function of the MZI, which is presented as a 'TE gain or insertion loss vs. Wavelength' graph, obtained from the simulation of an MZI with path lengths of 100 µm and 200 µm (ΔL = 100 µm) using Ansys INTERCONNECT.

3.4 MZI Simulation (Free Spectral Range): Another feature which is calculated from the functioning of an MZI is the free spectral range (FSR) which means the linear spacing between the adjacent maxima or minima of an MZI transmission spectra at various wavelengths.

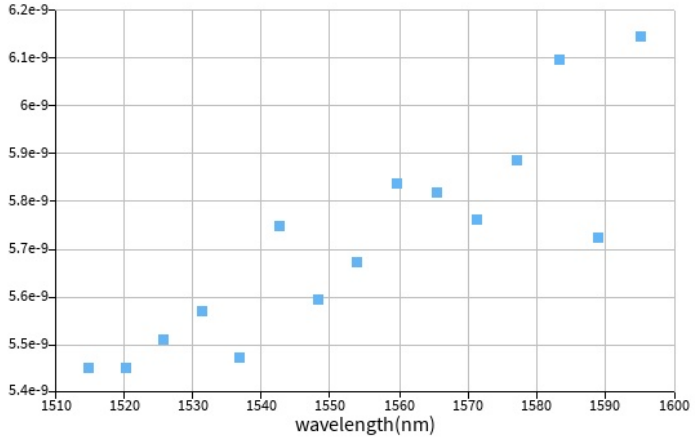

Figure 9: Free Spectral Range (FSR) obtained from the above simulation in Ansys INTERCONNECT using the model waveguide LDF file generated after eigenmode solving in MODE.

In simple terms, FSR is the spacing between adjacent peaks of a light wave. In an imbalanced MZI, it means the recurring distances at which constructive or destructive interferences occur as the two phase shifted light waves couple back, and can be calculated from group index using the following equation:

$$\mathrm{FSR} = \frac{\lambda^2}{n_g \cdot \Delta L} \qquad \text{(eq. 12)}$$

4. Fabrication

Before fabrication, the MZIs are designed in KLayout using the SiEPIC and EBeam component libraries. SiEPIC is used for designing within the scope of the standard silicon-on-insulator (SOI) platform with 220 nm silicon thickness, while EBeam is used for designing within the scope of the electron beam lithography based rapid prototyping. Afterwards, all the designs are verified, submitted, and sent out for fabrication.

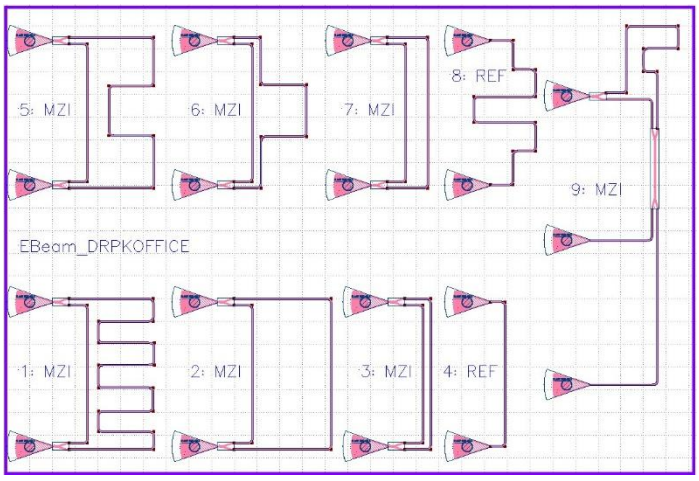

Figure 10: Layout of the 9 photonic circuits to be fabricated designed with KLayout. There are 6 imbalanced MZIs, 1 imbalanced MZI with a broadband 50-50 directional coupler, and 2 reference waveguides with input-output grating couplers.

Table 2: Designed MZIs, their waveguide lengths, and their waveguide path length differences.

Type	Waveguide Lengths (µm)
1: MZI	550, 150, (ΔL = 400)
2: MZI	300, 150, (ΔL = 150)
3: MZI	175, 150, (ΔL = 025)
4: Reference	150
5: MZI	350, 150, (ΔL = 200)
6: MZI	250, 150, (ΔL = 100)
7: MZI	200, 150, (ΔL = 050)
8: Reference	300
9: MZI with a 50-50 DC	244.318, 64.318 (ΔL= 180)

4.1 Washington Nanofabrication Facility (WNF) silicon photonics process.

The devices were fabricated using 100 keV Electron Beam Lithography [5]. The fabrication used silicon-on-insulator wafer with 220 nm thick silicon on 3 µm thick silicon dioxide. The substrates were 25 mm squares diced from 150 mm wafers. After a solvent rinse and hot-plate dehydration bake, hydrogen silsesquioxane resist (HSQ, Dow-Corning XP-1541-006) was spin-coated at 4000 rpm, then hotplate baked at 80 °C for 4 minutes. Electron beam lithography was performed using a JEOL JBX-6300FS system operated at 100 keV energy, 8 nA beam current, and 500 µm exposure field size. The machine grid used for shape placement was 1 nm, while the beam stepping grid, the spacing between dwell points during the shape writing, was 6 nm. An exposure dose of 2800 µC/cm^2 was used. The resist was developed by immersion in 25% tetramethylammonium hydroxide for 4 minutes, followed by a flowing deionized water rinse for 60 s, an isopropanol rinse for 10 s, and then blown dry with nitrogen. The silicon was removed from unexposed areas using inductively coupled plasma etching in an Oxford

Plasmalab System 100, with a chlorine gas flow of 20 sccm, pressure of 12 mT, ICP power of 800 W, bias power of 40 W, and a platen temperature of 20 °C, resulting in a bias voltage of 185 V. During etching, chips were mounted on a 100 mm silicon carrier wafer using perfluoropolyether vacuum oil.

4.2 Applied Nanotools, Inc. NanoSOI process

The photonic devices were fabricated using the NanoSOI MPW fabrication process by Applied Nanotools Inc. (http://www.appliednt.com/nanosoi; Edmonton, Canada) which is based on direct-write 100 keV electron beam lithography technology. Silicon-on-insulator wafers of 200 mm diameter, 220 nm device thickness and 2 µm buffer oxide thickness are used as the base material for the fabrication. The wafer was pre-diced into square substrates with dimensions of 25x25 mm, and lines were scribed into the substrate backsides to facilitate easy separation into smaller chips once fabrication was complete. After an initial wafer clean using piranha solution (3:1 H2SO4:H2O2) for 15 minutes and water/IPA rinse, hydrogen silsesquioxane (HSQ) resist was spin-coated onto the substrate and heated to evaporate the solvent. The photonic devices were patterned using a Raith EBPG 5000+ electron beam instrument using a raster step size of 5 nm. The exposure dosage of the design was corrected for proximity effects that result from the backscatter of electrons from exposure of nearby features. Shape writing order was optimized for efficient patterning and minimal beam drift. After the e-beam exposure and subsequent development with a tetramethylammonium sulfate (TMAH) solution, the devices were inspected optically for residues and/or defects. The chips were then mounted on a 4" handle wafer and underwent an anisotropic ICP-RIE etch process using chlorine after qualification of the etch rate. The resist was removed from the surface of the devices using a 10:1 buffer oxide wet etch, and the devices were inspected using a scanning electron microscope (SEM) to verify patterning and etch quality. A 2.2 µm oxide cladding was deposited using a plasma-enhanced chemical vapour deposition (PECVD) process based on tetraethyl orthosilicate (TEOS) at 300ºC. Reflectometry measurements were performed throughout the process to verify the device layer, buffer oxide and cladding thicknesses before delivery.

5. Experimental Data

To characterize the devices, a custom-built automated test setup [6, 10] with automated control software written in Python was used [7]. An Agilent 81600B tunable laser was used as the input source and Agilent 81635A optical power sensors as the output detectors. The wavelength was swept from 1500 to 1600 nm in 10 pm steps. A polarization maintaining (PM) fibre was used to maintain the polarization state of the light, to couple the TE polarization into the grating couplers [8]. A 90º rotation was used to inject light into the TM grating couplers [8]. A polarization maintaining fibre array was used to couple light in/out of the chip [9]. Plots of experimental data were generated using a built-in MATLAB interpreter.

6. Data Analysis

The objective of the following data analysis is to learn the methods of baseline correction, calibration, curve fitting of MZI transfer function, calculating group index and FSR, etc., and subsequently match the data outputs of fabricated MZIs to those of the simulated MZIs, in particular their transfer function profiles, group indices, and FSRs.

6.1 Baseline Correction: The grating couplers have a finite size and a specific shape and, as a result, finite bandwidth which causes variable insertion loss across a wavelength sweep measurement. This variable insertion loss also gets superimposed in the transmission spectra of an MZI during its wavelength sweep measurement. Removing this grating coupler induced deformity is what the baseline correction performed for. It is done by fitting the MZI transmission output graph to a low-order polynomial (for example, order value 4). This polynomial fit curve is then subtracted from the graph to get the flattened transmission spectra. This method however does not give the real insertion loss of the MZI.

6.2 Calibration with a Reference Waveguide-GC device: Calibration can also be called as another method of baseline correction and it is done by obtaining the real output of an on-chip reference waveguide-GC device (2 GCs connected by a waveguide), curve fitting it using a low-order polynomial to remove noise, and then subtracting this output from the transmission spectra output of the MZIs. This gives the flattened transmission spectra of the MZIs due to the removal of the spectra-deforming effects of GCs, waveguide lengths and waveguide bends. The reference device should be on the same chip and very closely located to the MZI to minimize manufacturing variabilities.

6.3 Curve Fitting: This is the next step after baseline correction or calibration. Here, the fabricated MZI output is assessed to obtain various parameters, such as group index, FSR, and dispersion parameter. The method of least squares is used here for curve fitting the measured MZI transfer function. The initial parameters for curve fitting need to be guessed and must be close enough to the unknown optimum values so that an initial curve fit can be obtained and then readjusted to achieve the best fit. A more robust method for finding more accurate initial fitting parameters is using automated tools to find peaks in the transmission spectra, calculating FSR values, calculating group indices to confirm the waveguide has low dispersion, finding mode number N with help from the simulated data, and then calculating the zeroth order n_1 which is then used for calculating the first order dispersion coefficient n_2. In summary, the automated tools first find the correct periodicity of the fitting curve and then horizontally shifts it to remove any offsets to get the best fit with the experimental data.

6.4 Data Matching: The measured transfer function, group index, and FSR are matched against their simulated equivalents. Similar values of these parameters indicate the accuracy of both simulation and the prototyping and experimental measurements.

6.5 Analysis of Measured & Simulated Data: Below given are the figures and plots generated for each of the 7 MZIs in the following serial order in each sub-section:

(a) KLayout schematic illustration of MZI (one figure).

(b) Simulated vs. Measured Transfer Function in same plot (one plot).

(c) Plot of Simulated FSR and Plot of Simulated Group Index (two plots).

(d) Plots of the Measured Data showing baseline-corrected transfer function, findpeaks based peak identification, free spectral range, waveguide group index, initial parameters based curve-fitted transfer function, fit parameters based curve-fitted transfer function, and the group index range (seven plots).

Table 3: Simulated (Sim) vs. Measured (Real) Group Indices and the percentage difference between them.

MZI	ΔL (μm)	Sim GI	Real GI	% Diff.
MZI 1	400	4.1944	4.1854	0.21
MZI 2	150	4.2080	4.1944	0.32
MZI 3	25	4.4961	4.2762	4.97
MZI 4 Ref	-	-	-	
MZI 5	200	4.2036	4.1735	0.72
MZI 6	100	4.2384	4.2347	0.09
MZI 7	50	4.3155	4.2912	0.57
MZI 8 Ref	-	-	-	
MZI 9 Ch1	180	4.1764	4.1643	0.29
MZI 9 Ch2	180	4.1842	4.1742	0.24

-- MZI 1 (ΔL = 400 μm) --

Measured Data

Mean Group Index estimate = 4.1854
Goodness of fit, r^2 value: 0.90925
Waveguide parameters at wavelength [um]: 1.5377
Group index: 4.1833
Dispersion [ps/nm/km]: 368.1109

Simulated Data

Mean Group Index = 4.1944

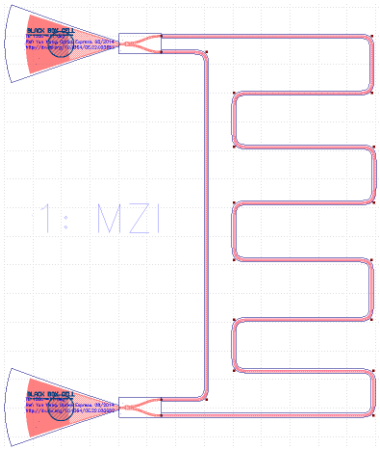

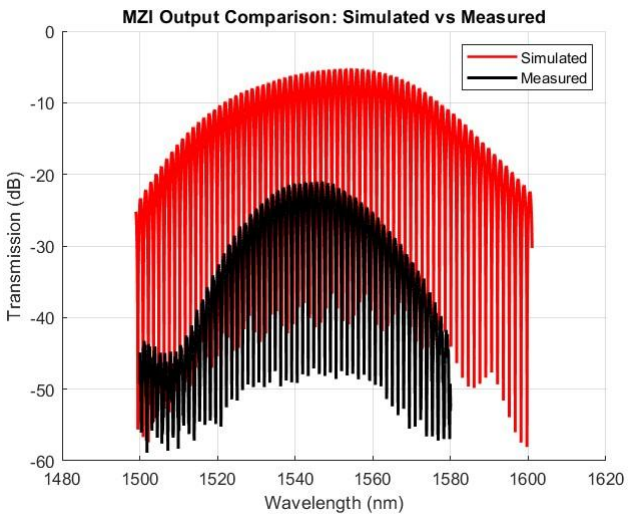

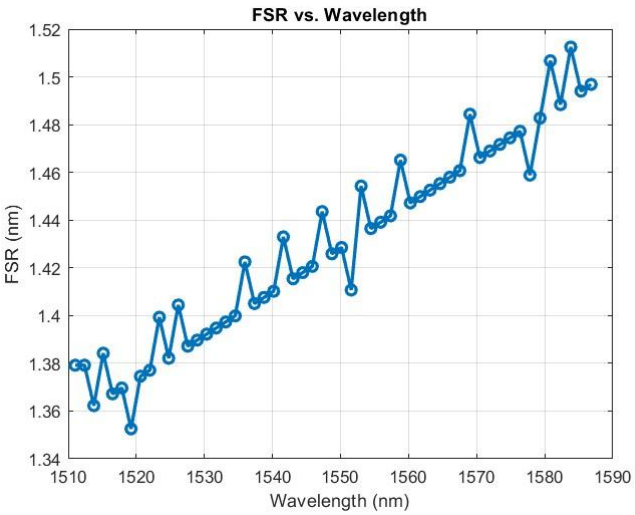

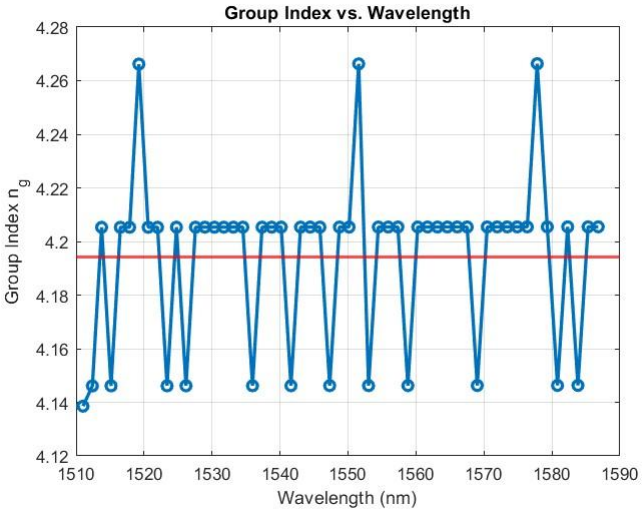

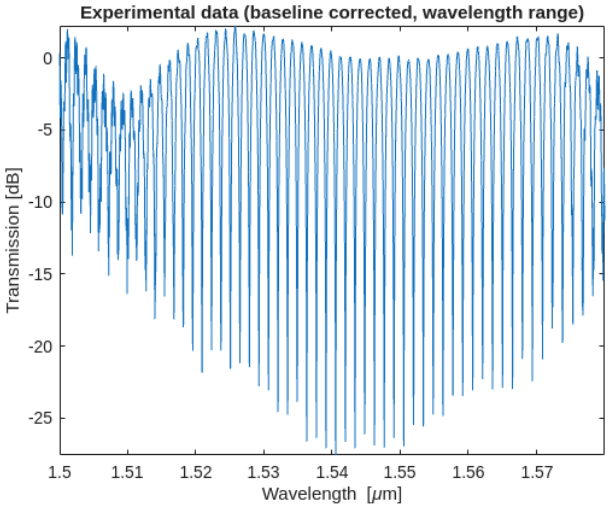

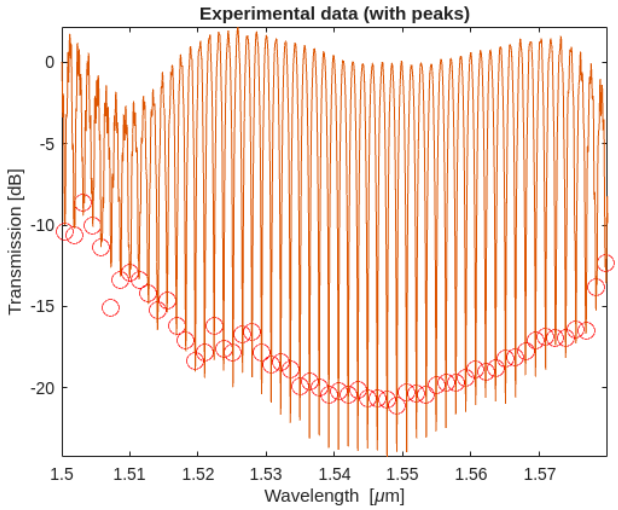

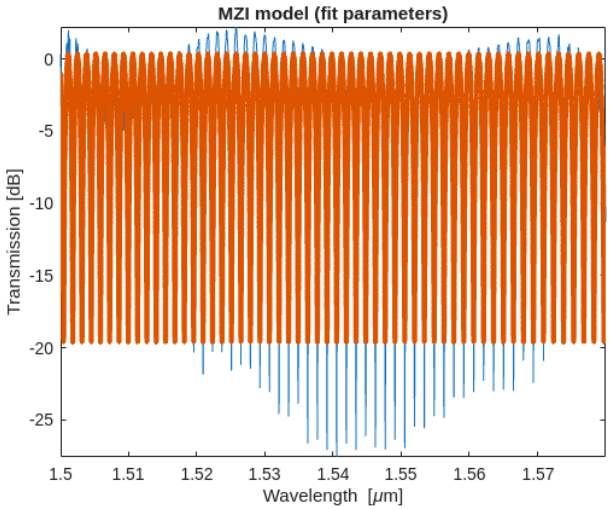

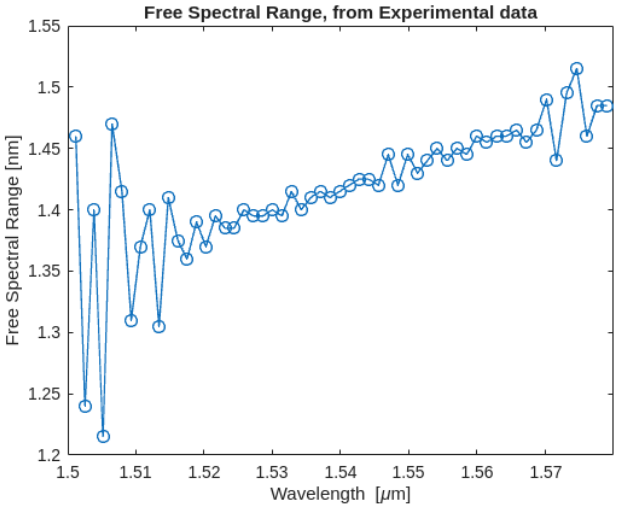

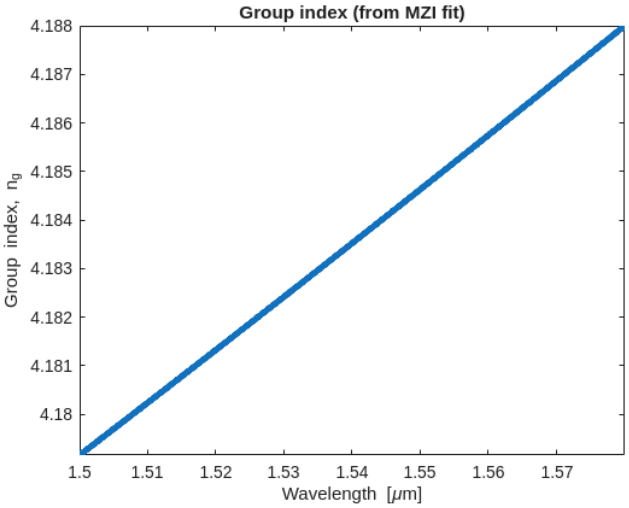

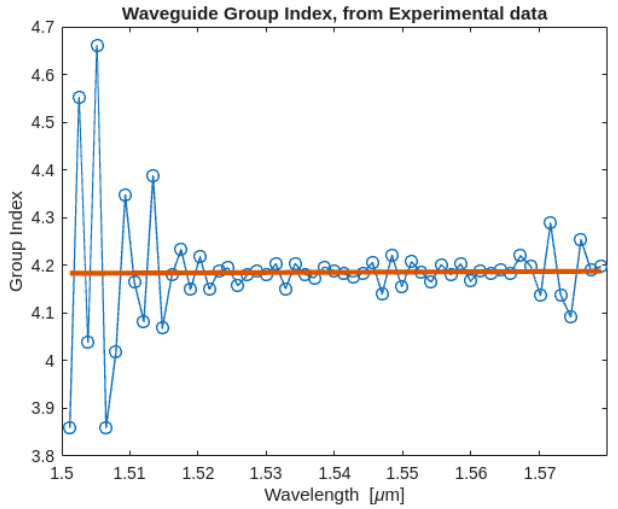

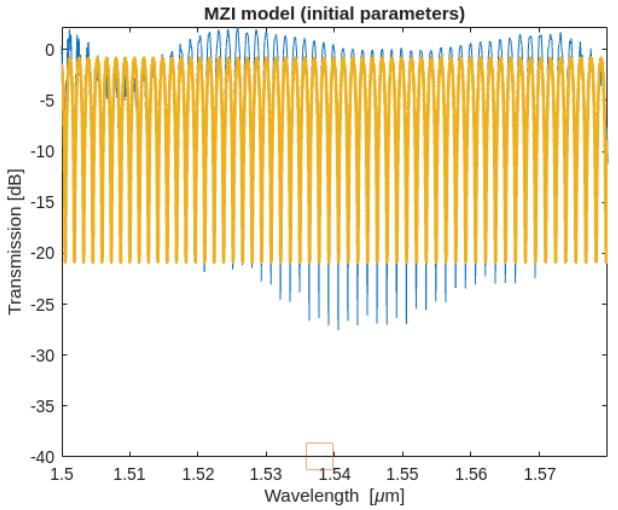

-- MZI 2 (ΔL = 150 μm) --

Measured Data

Mean Group Index estimate = 4.1944
Goodness of fit, r^2 value: 0.91435
Waveguide parameters at wavelength [um]: 1.5369
Group index: 4.1762
Dispersion [ps/nm/km]: 1285.7142

Simulated Data

Mean Group Index = 4.2080

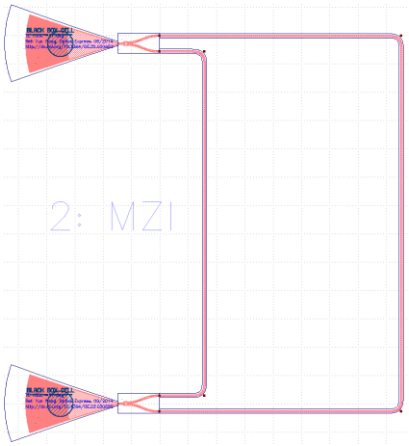

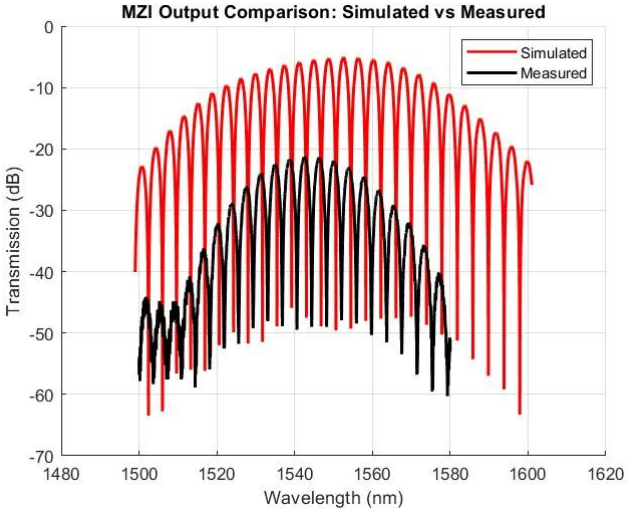
MZI Output Comparison: Simulated vs Measured
Simulated
Measured
Transmission (dB)
Wavelength (nm)

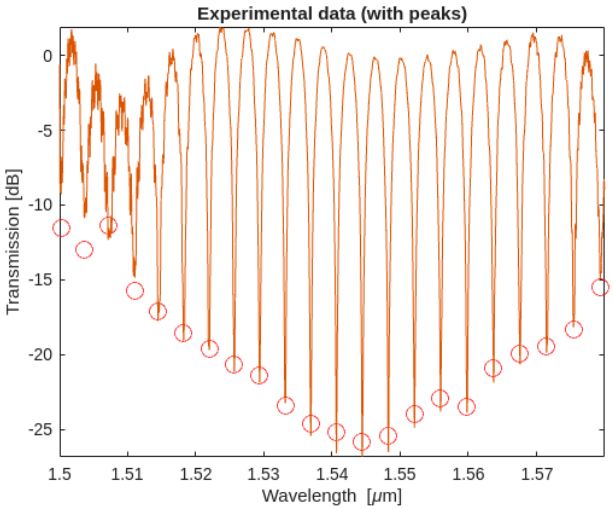
Experimental data (with peaks)
Transmission [dB]
Wavelength [μm]

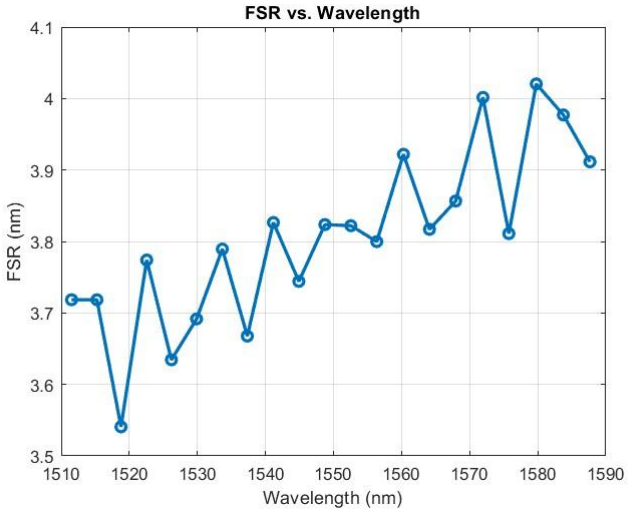
FSR vs. Wavelength
FSR (nm)
Wavelength (nm)

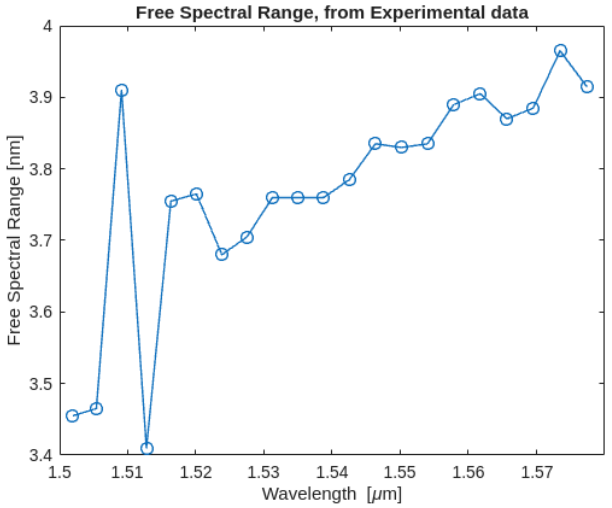
Free Spectral Range, from Experimental data
Free Spectral Range [nm]
Wavelength [μm]

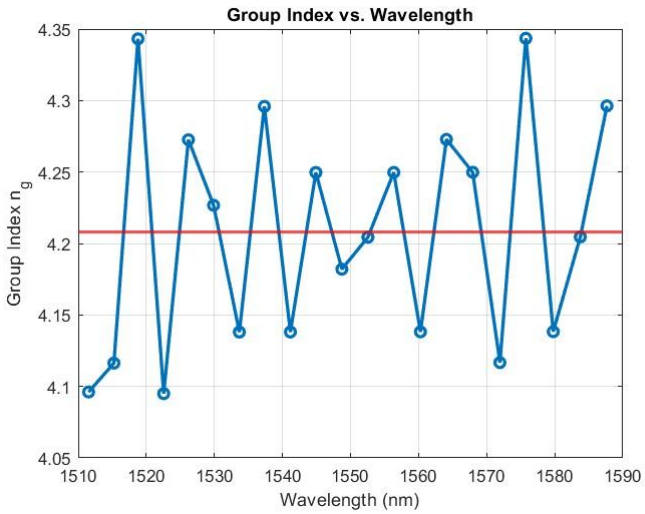
Group Index vs. Wavelength
Group Index n_g
Wavelength (nm)

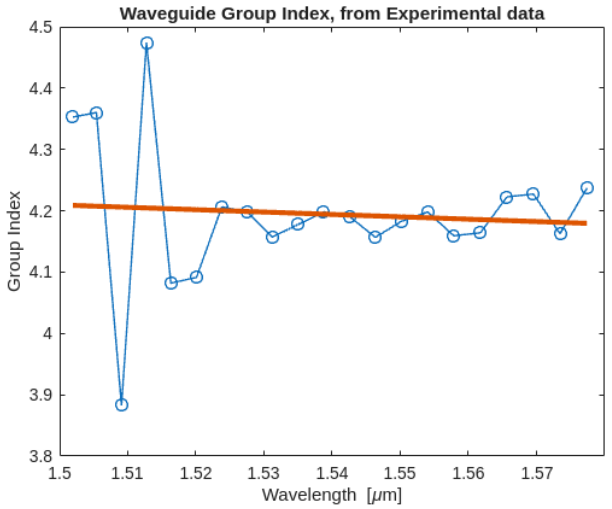
Waveguide Group Index, from Experimental data
Group Index
Wavelength [μm]

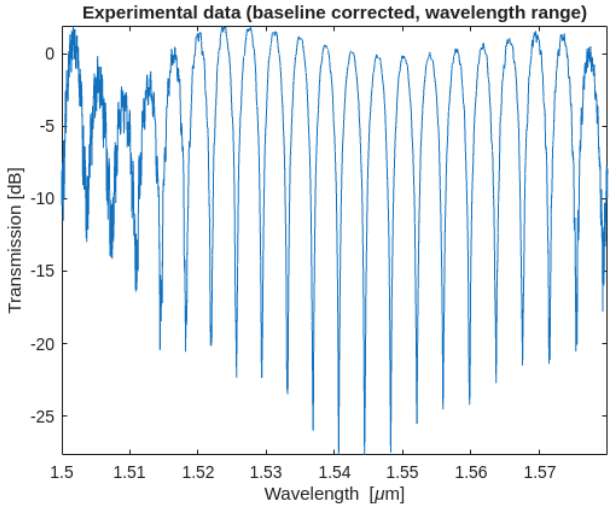
Experimental data (baseline corrected, wavelength range)
Transmission [dB]
Wavelength [μm]

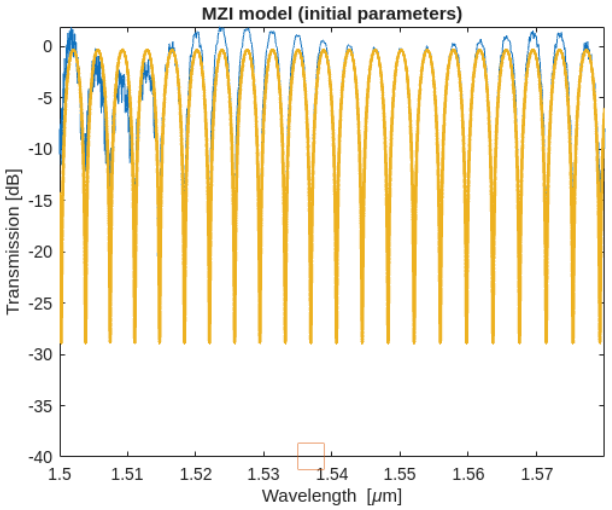
MZI model (initial parameters)
Transmission [dB]
Wavelength [μm]

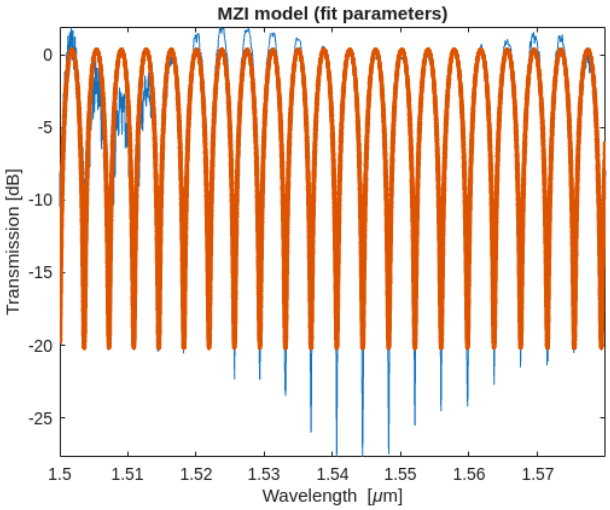

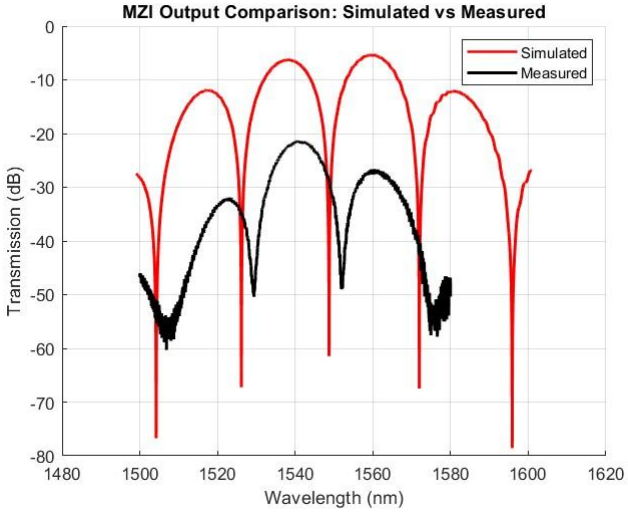

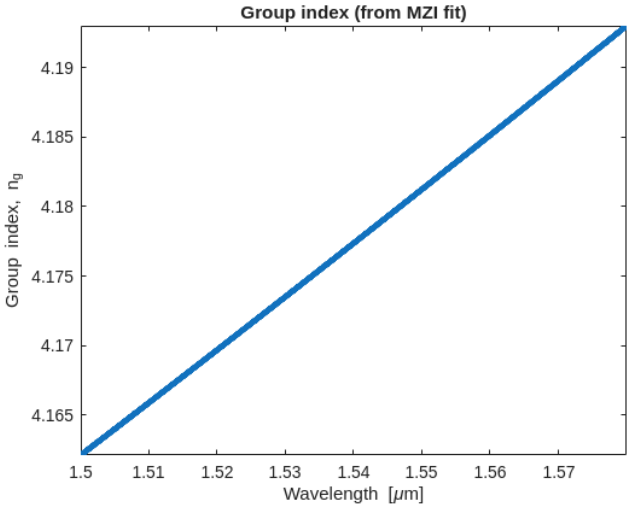

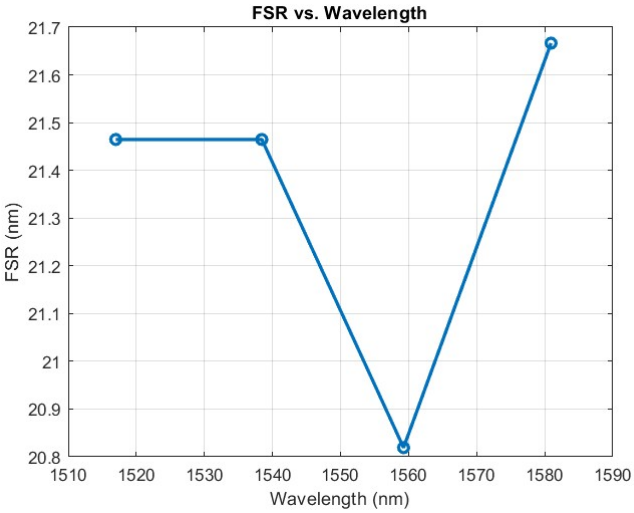

-- MZI 3 (ΔL = 25 μm) --

Measured Data

Mean Group Index estimate = 4.2762
Goodness of fit, r^2 value: 0.84954
Waveguide parameters at wavelength [um]: 1.5777
Group index: 4.1914
Dispersion [ps/nm/km]: -4714.8856

Simulated Data

Mean Group Index = 4.4961

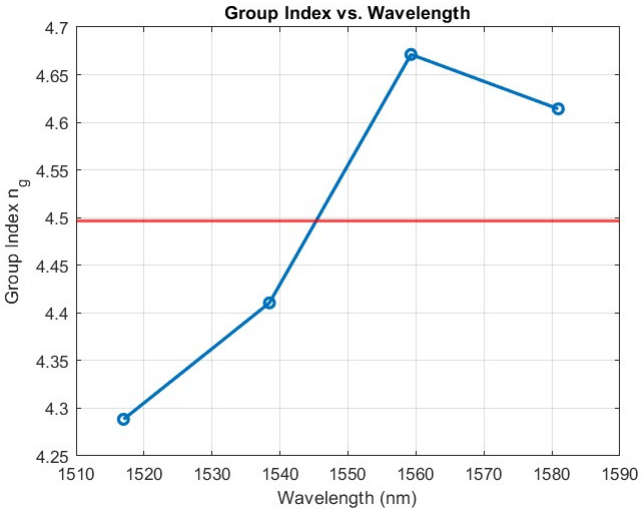

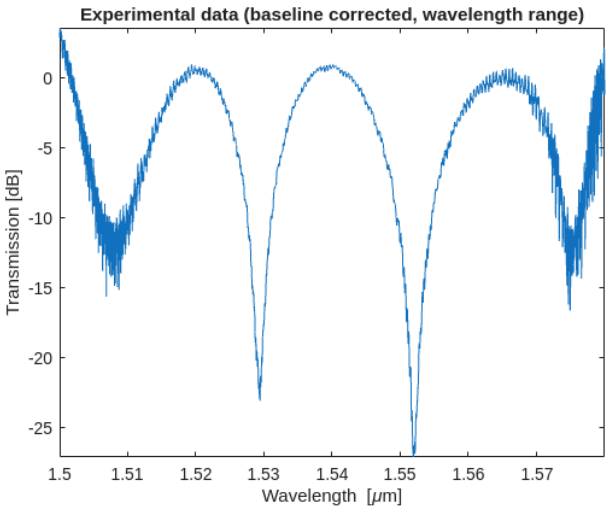

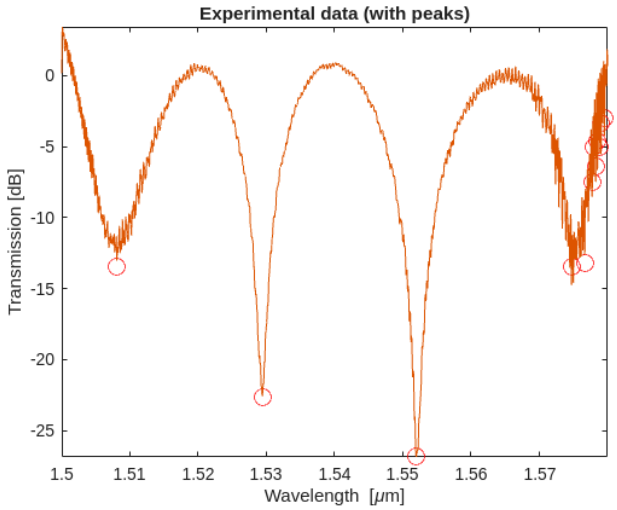

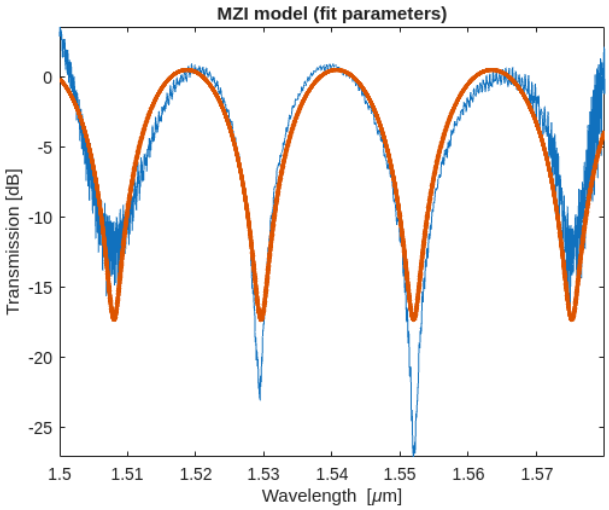

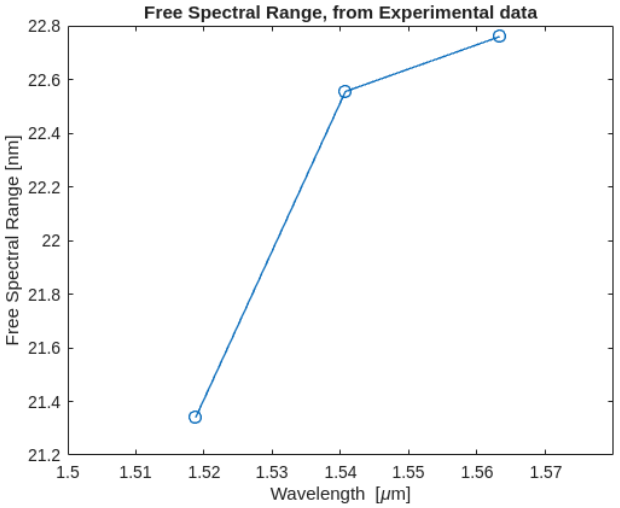

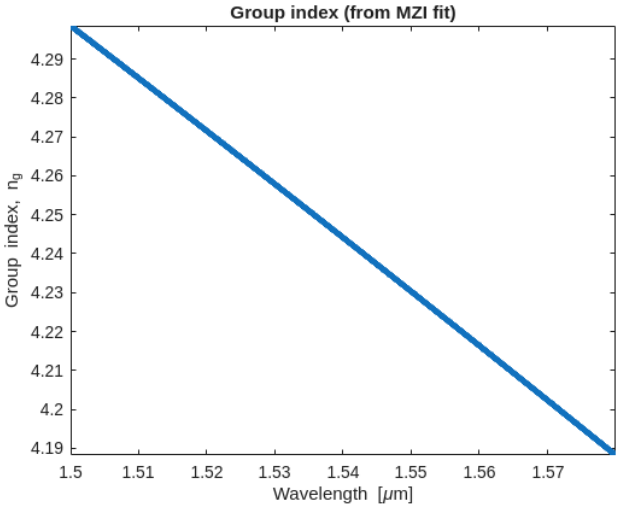

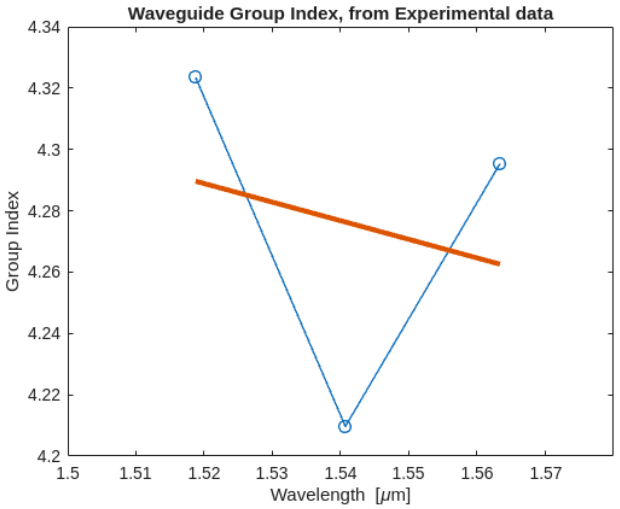

-- MZI 4 --

Reference Device.

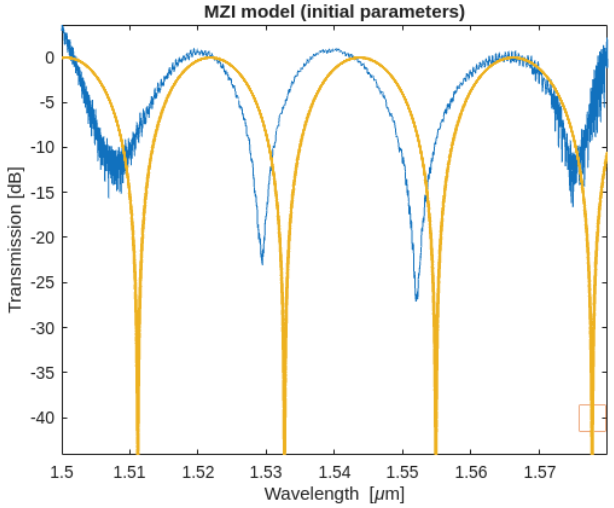

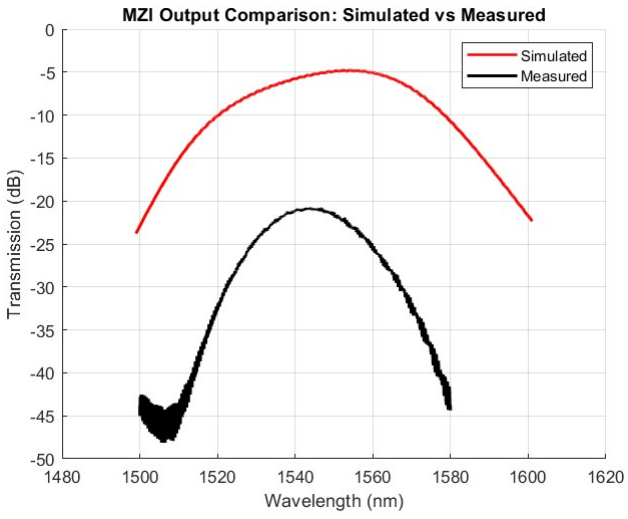

-- MZI 5 (ΔL = 200 μm) --

Measured Data

Mean Group Index estimate = 4.1735
Goodness of fit, r^2 value: 0.88608
Waveguide parameters at wavelength [um]: 1.5286
Group index: 4.1767
Dispersion [ps/nm/km]: 799.8447

Simulated Data

Mean Group Index = 4.2036

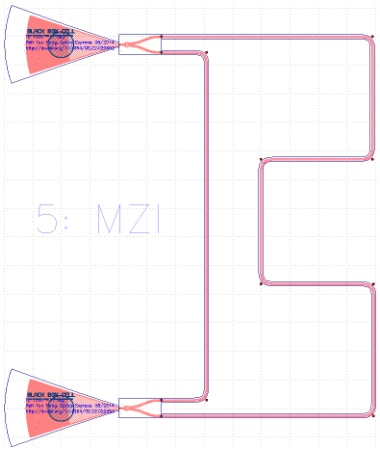

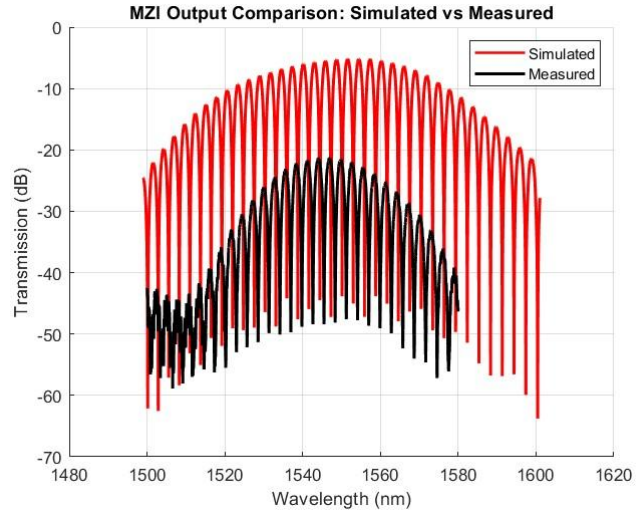

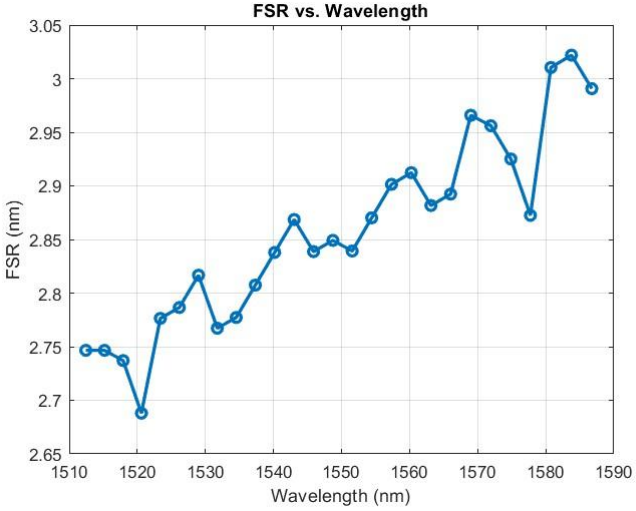

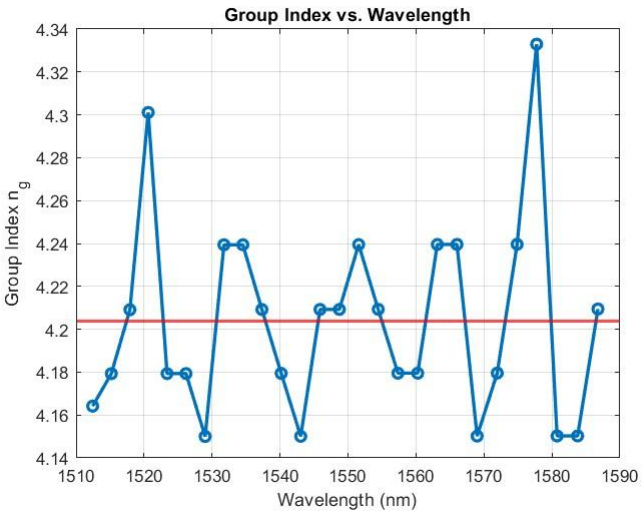

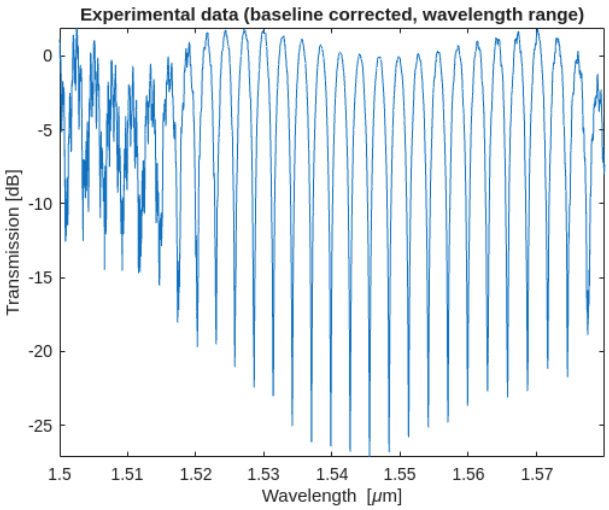

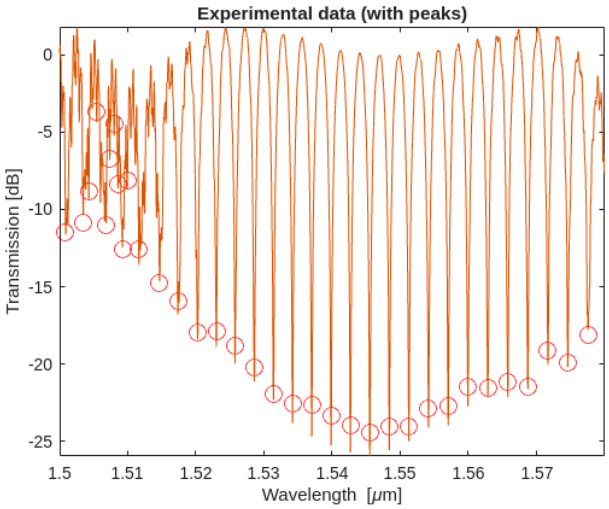

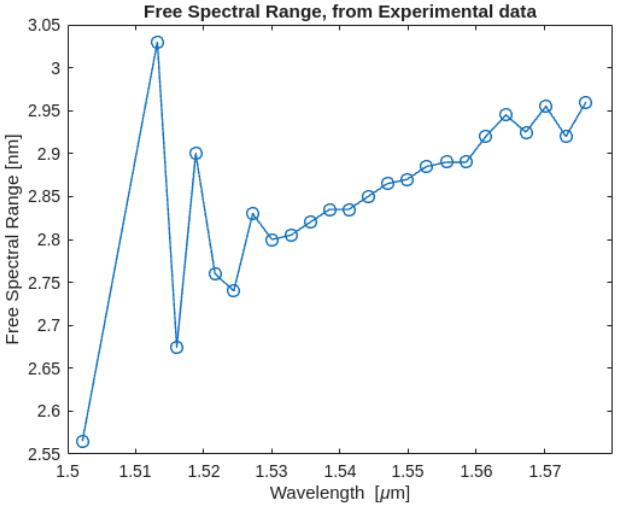

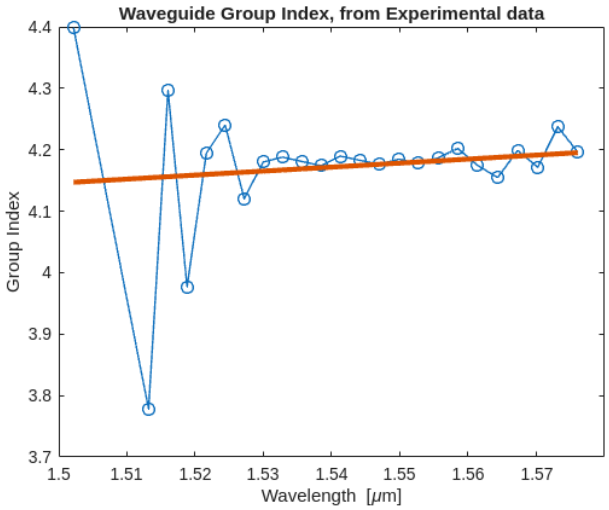

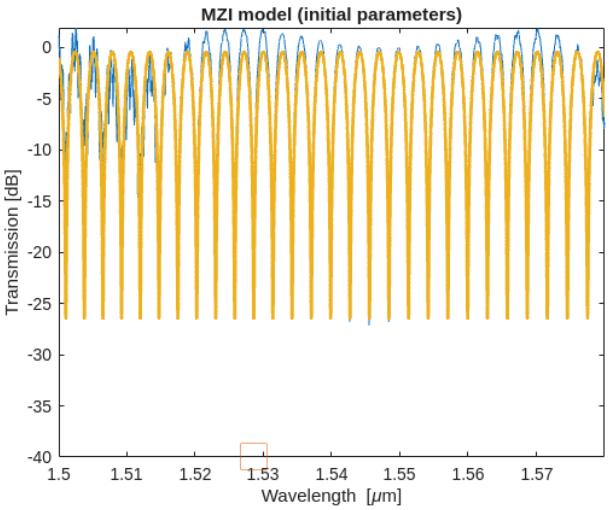

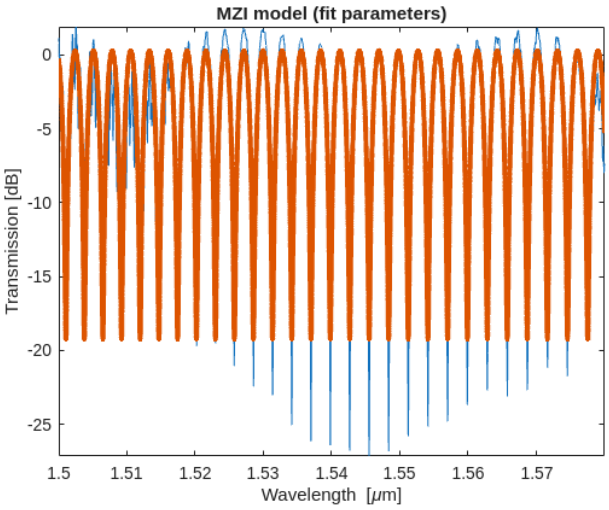

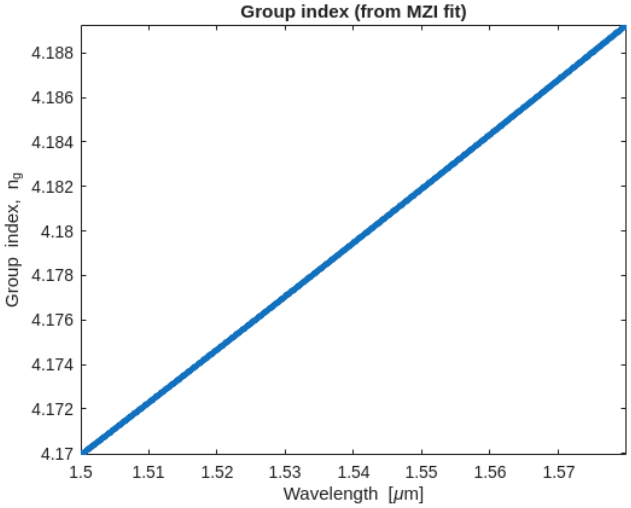

-- MZI 6 (ΔL = 100 μm) --

Measured Data

Mean Group Index estimate = 4.2347
Goodness of fit, r^2 value: 0.89135
Waveguide parameters at wavelength [um]: 1.5185
Group index: 4.1796
Dispersion [ps/nm/km]: 560.5597

Simulated Data

Mean Group Index = 4.2384

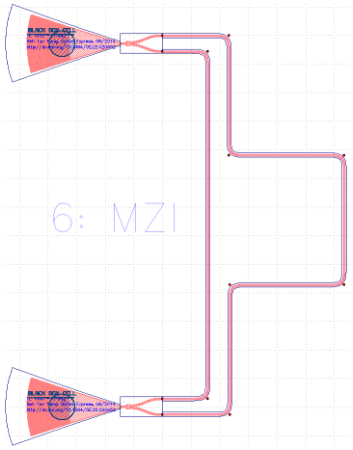

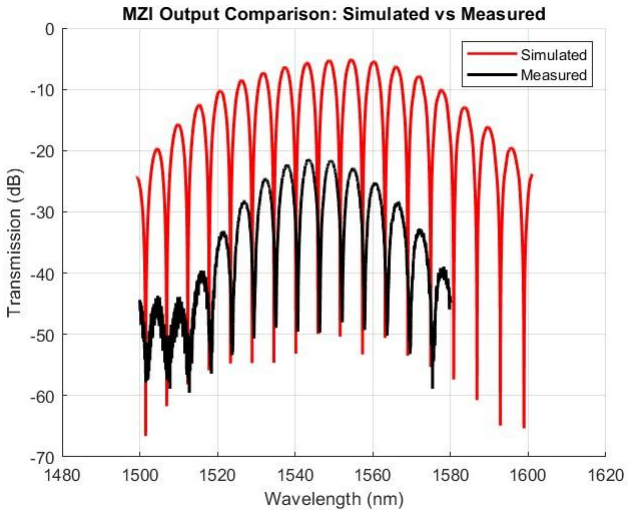

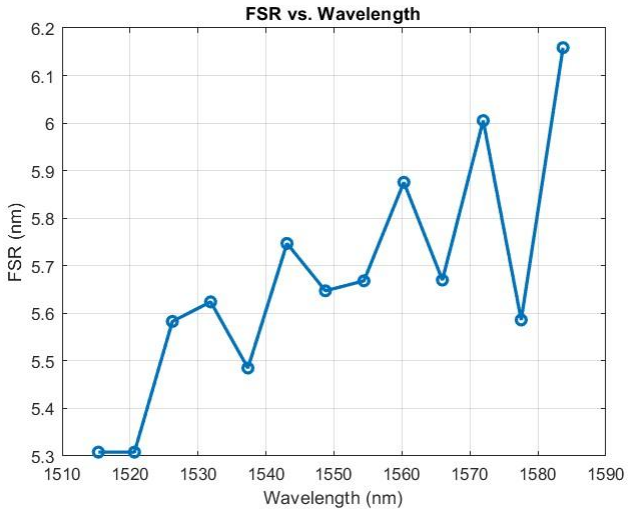

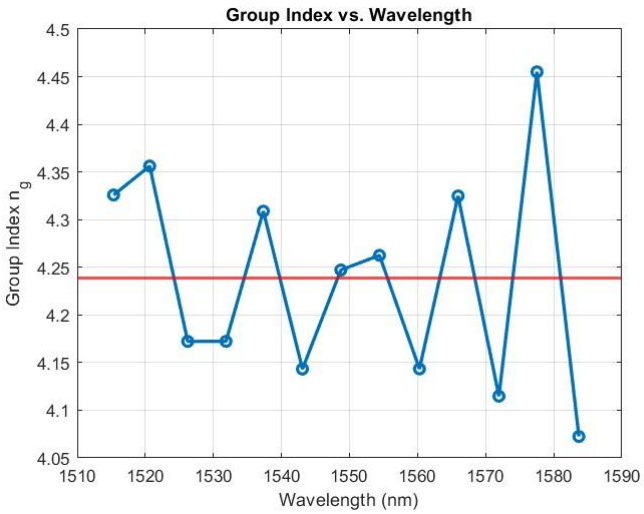
Group Index vs. Wavelength
Group Index n_g
Wavelength (nm)

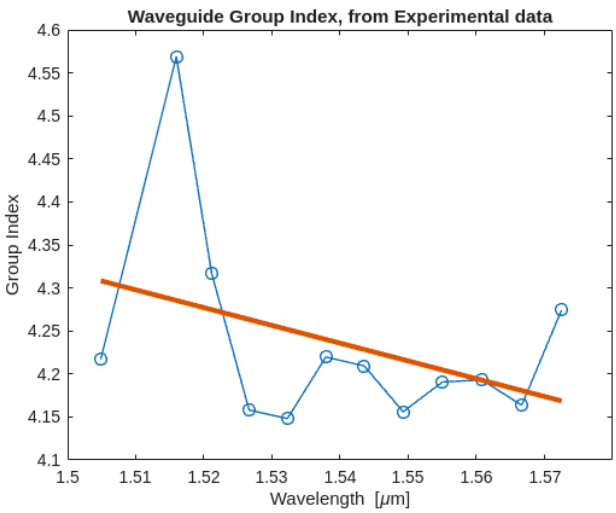
Waveguide Group Index, from Experimental data
Group Index
Wavelength [μm]

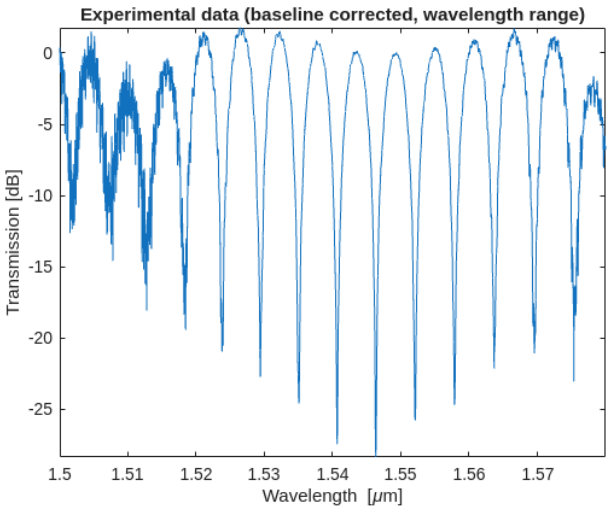
Experimental data (baseline corrected, wavelength range)
Transmission [dB]
Wavelength [μm]

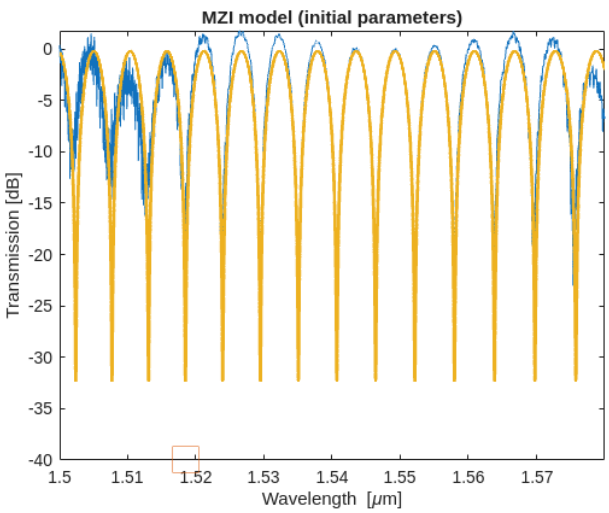
MZI model (initial parameters)
Transmission [dB]
Wavelength [μm]

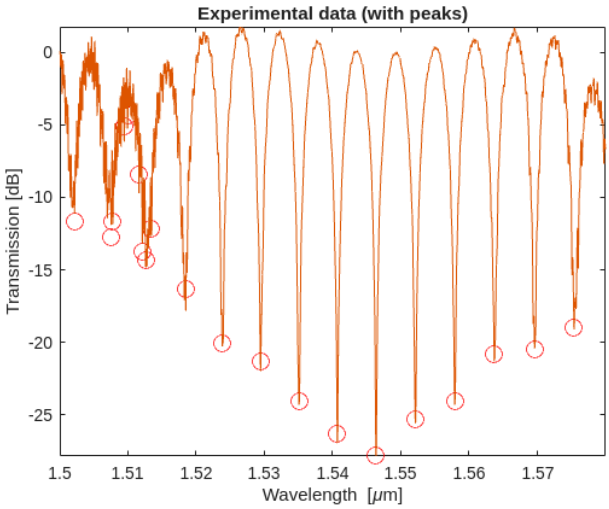
Experimental data (with peaks)
Transmission [dB]
Wavelength [μm]

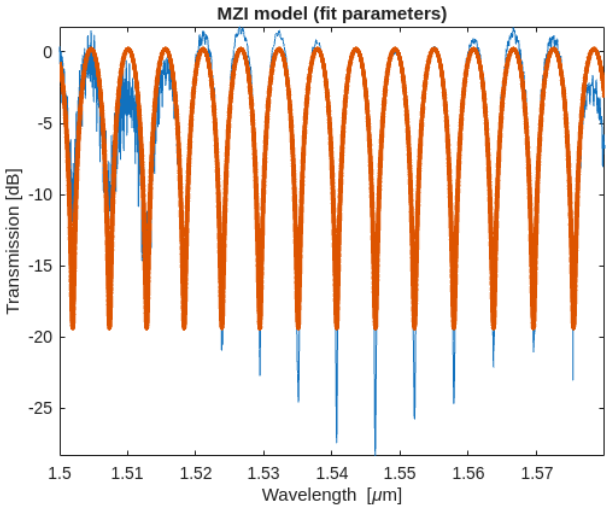
MZI model (fit parameters)
Transmission [dB]
Wavelength [μm]

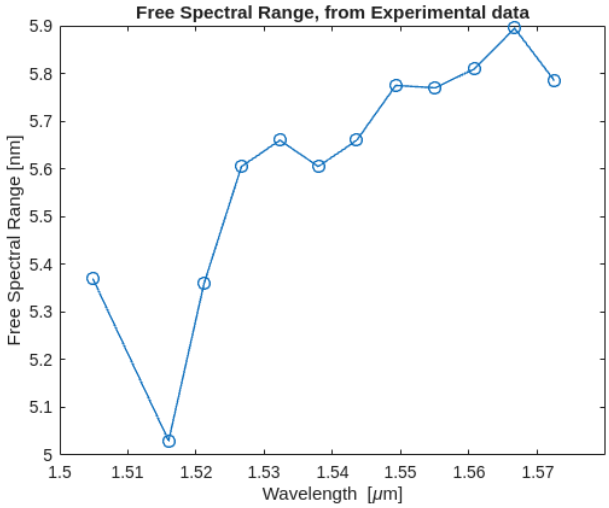
Free Spectral Range, from Experimental data
Free Spectral Range [nm]
Wavelength [μm]

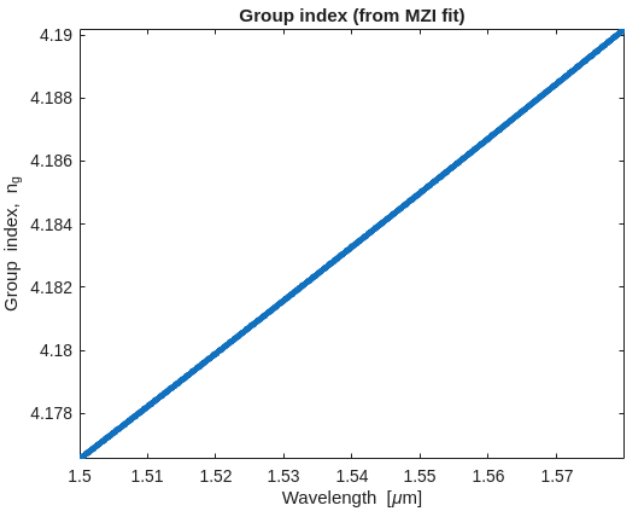
Group index (from MZI fit)
Group index, n_g
Wavelength [μm]

-- MZI 7 (ΔL = 50 μm) --

Measured Data

Mean Group Index estimate = 4.2912
Goodness of fit, r^2 value: 0.89573
Waveguide parameters at wavelength [um]: 1.5455
Group index: 4.1548
Dispersion [ps/nm/km]: 15838.4141

Simulated Data

Mean Group Index = 4.3155

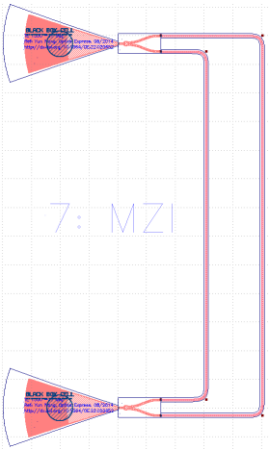

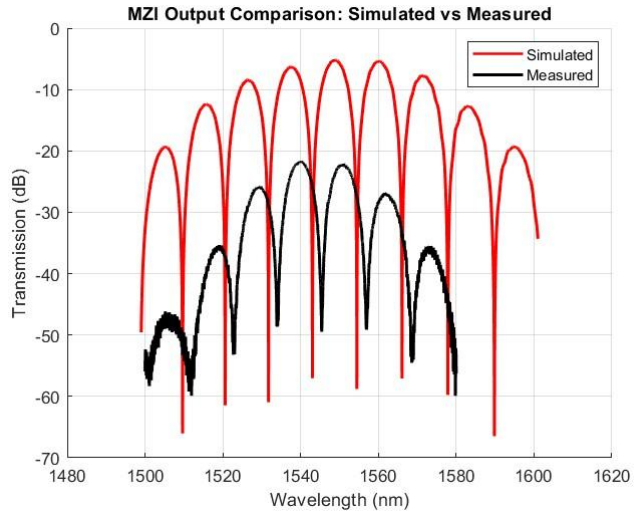

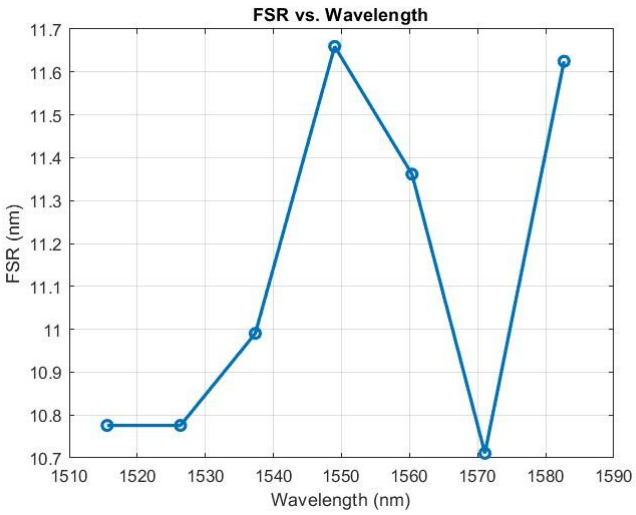

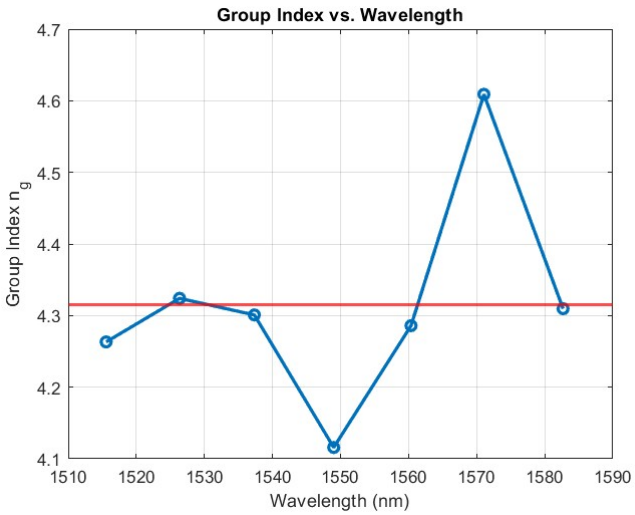

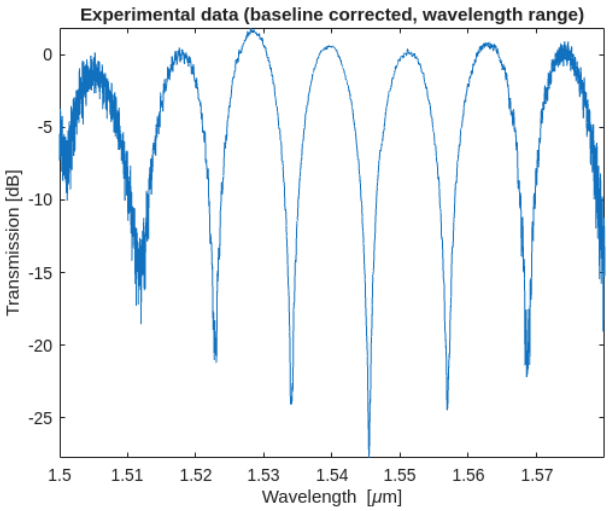

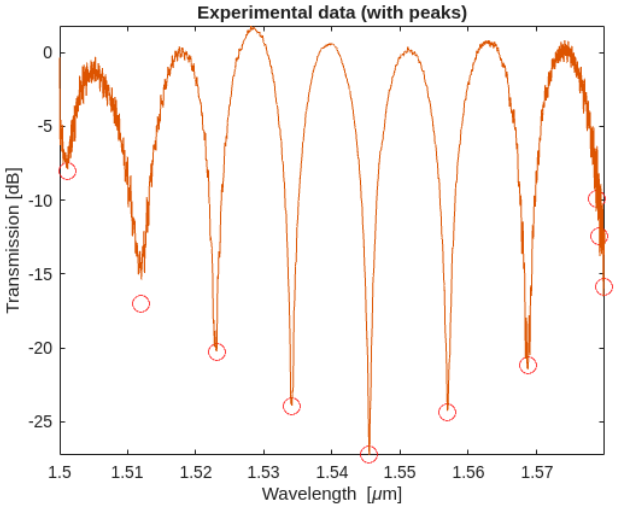

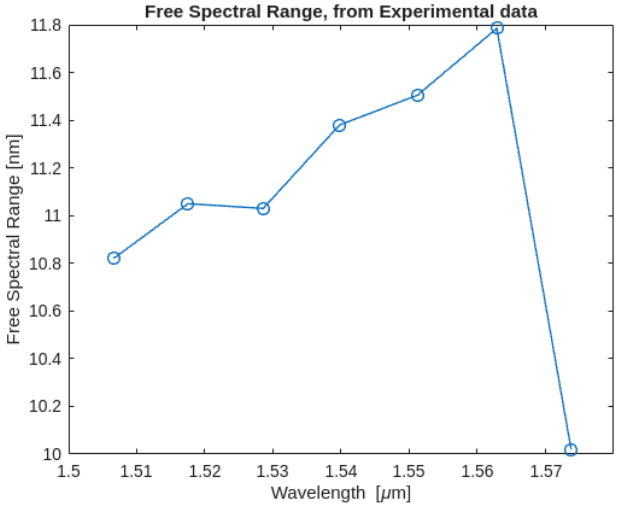

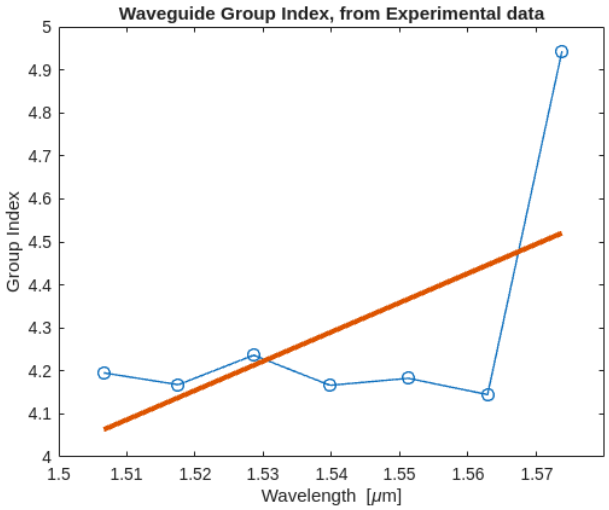

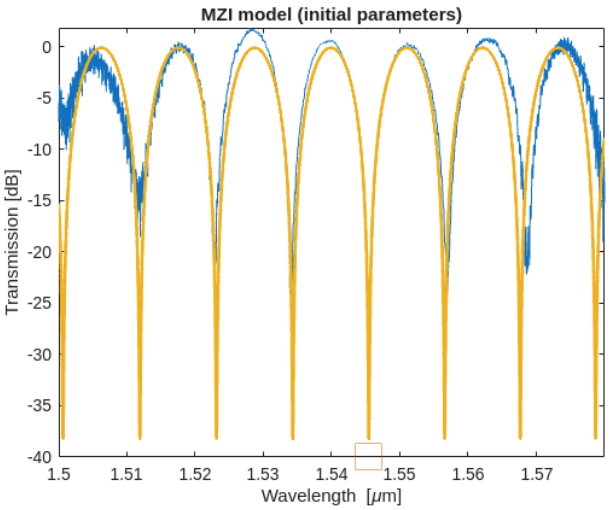

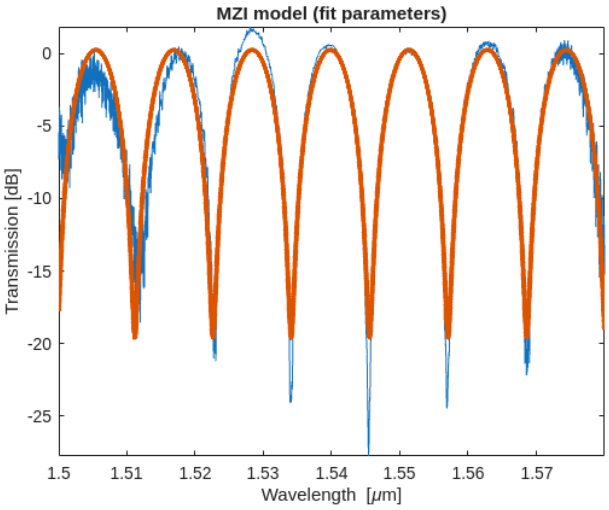

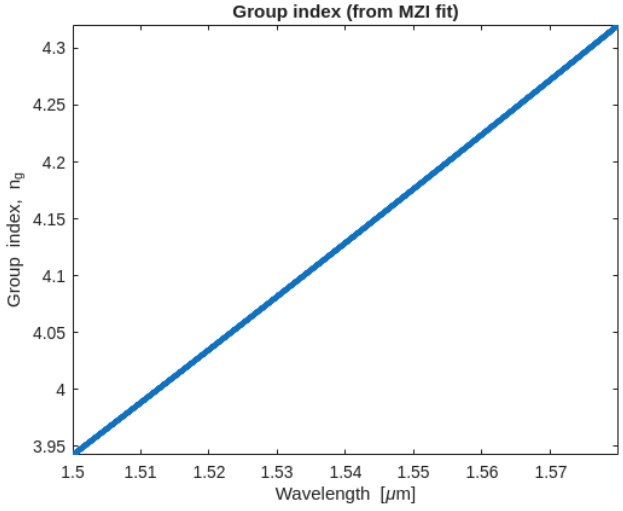

-- MZI 8 --

Reference Device.

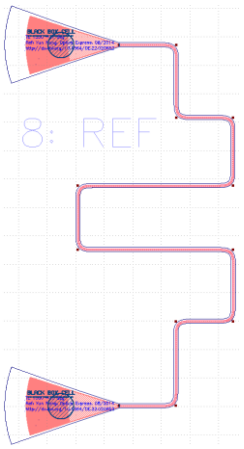

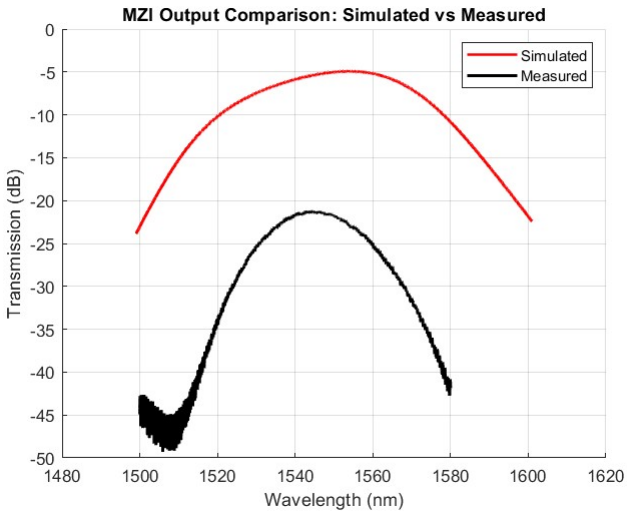

-- MZI 9 (ΔL = 180 μm) with a DC --

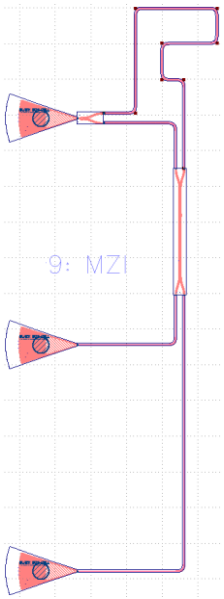

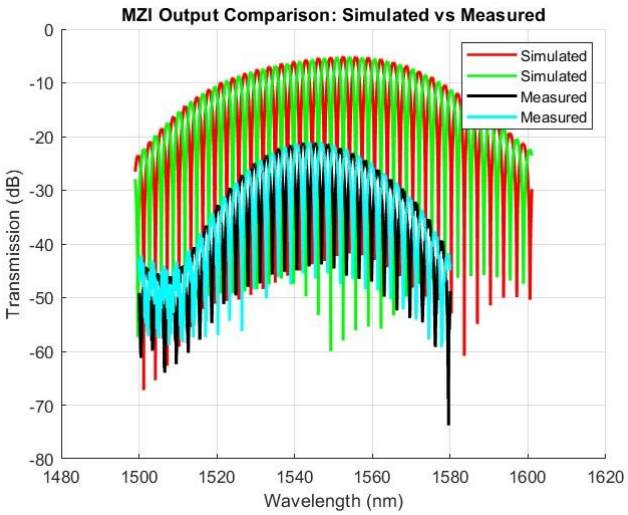

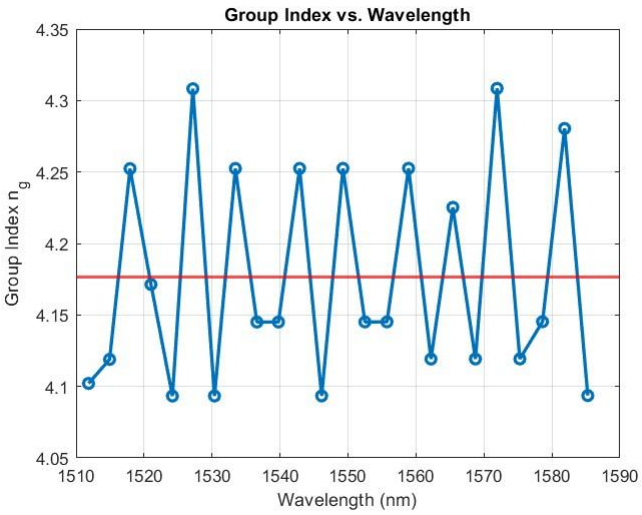

Measured Data from Output Grating Coupler 1
Mean Group Index estimate = 4.1643
Goodness of fit, r^2 value: 0.93322
Waveguide parameters at wavelength [um]: 1.5374
Group index: 4.1641
Dispersion [ps/nm/km]: -121.2521

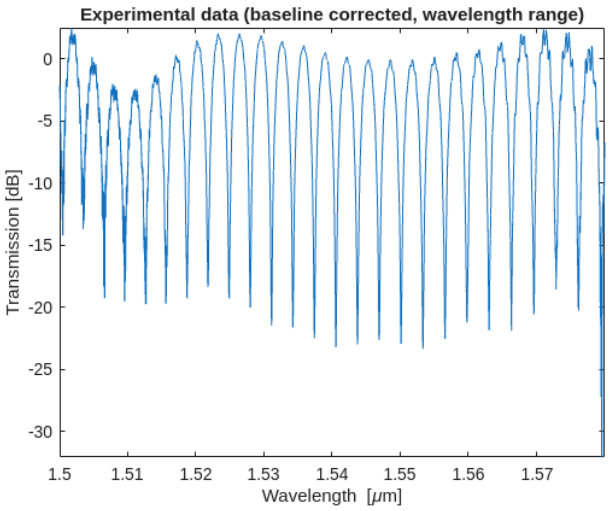

Simulated Data from Output Grating Coupler 1
Mean Group Index = 4.1764

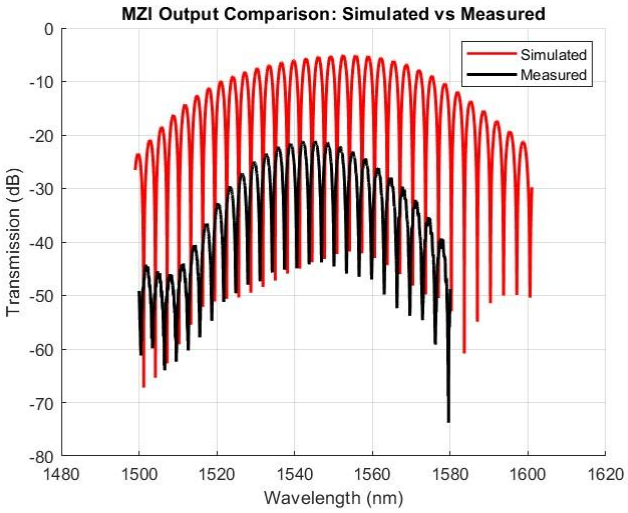

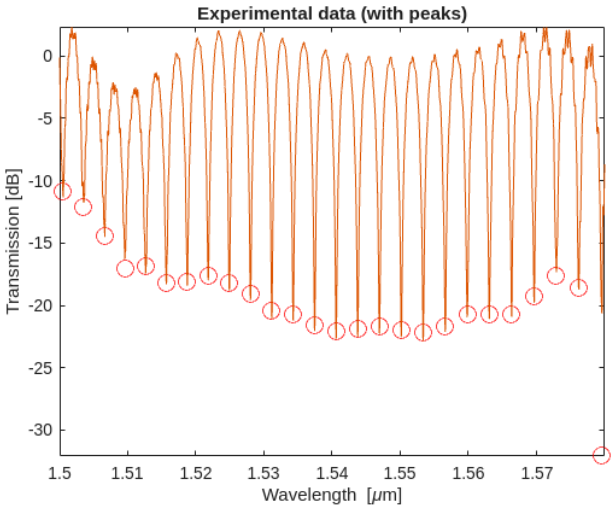

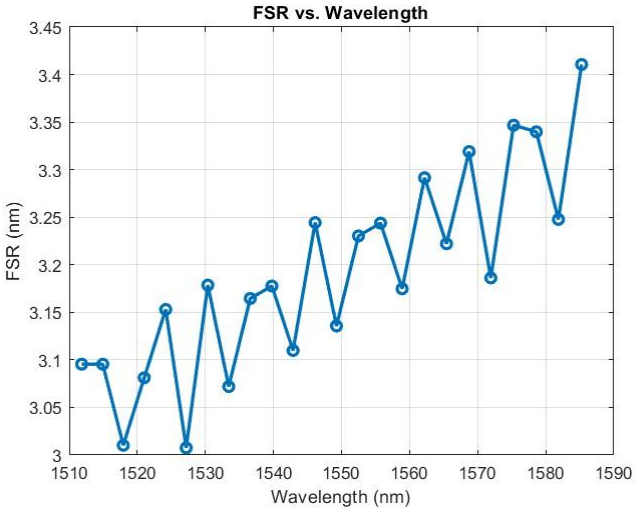

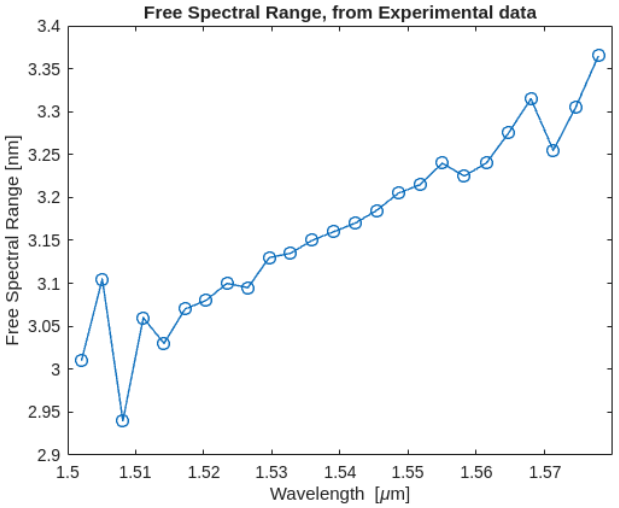

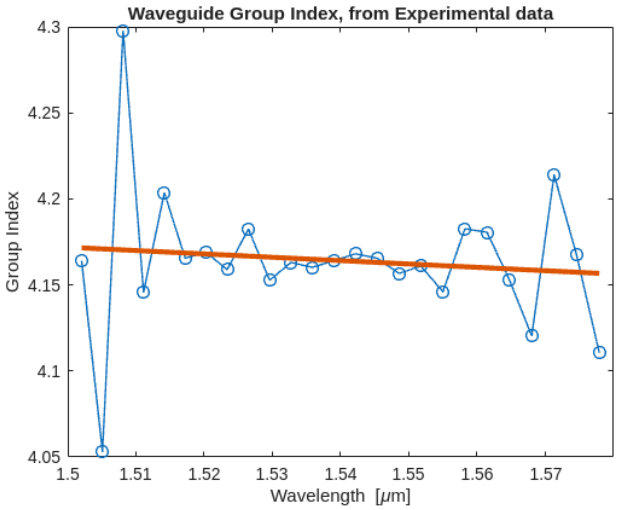

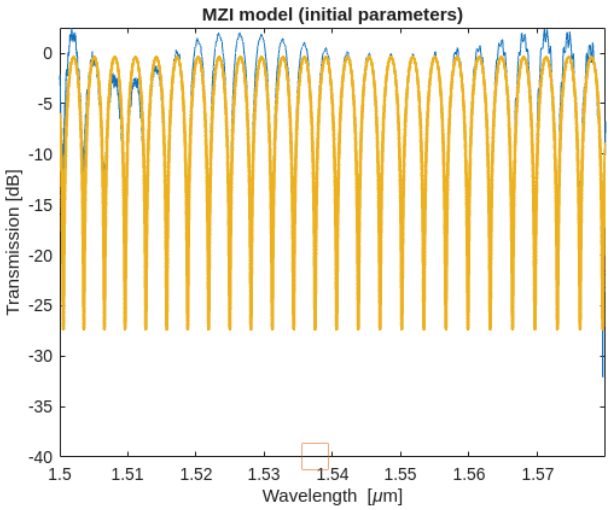

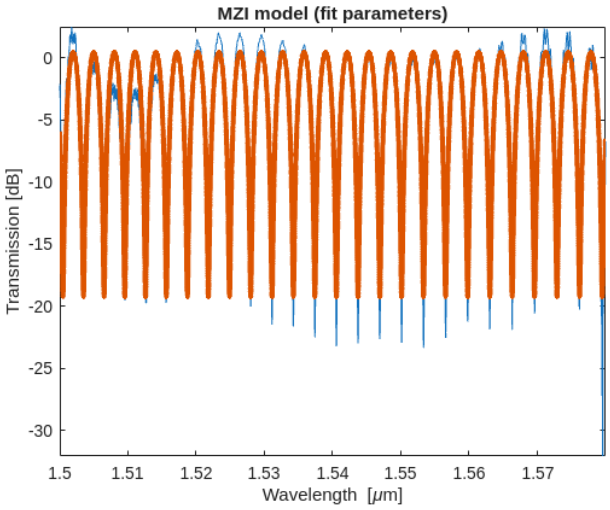

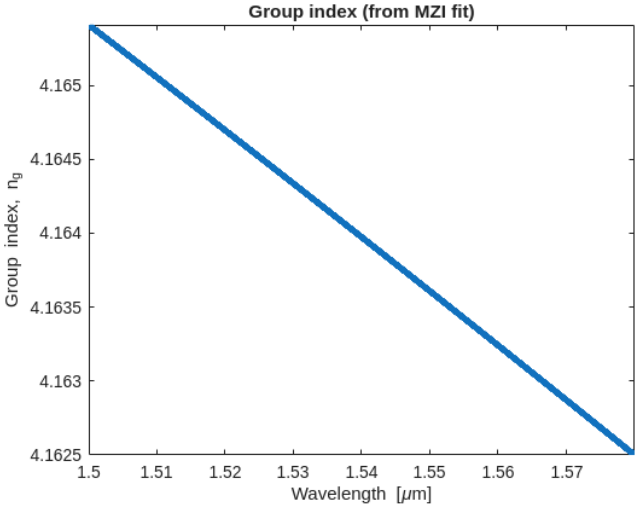

Measured Data from Output Grating Coupler 2
Mean Group Index estimate: 4.1742
Goodness of fit, r^2 value: 0.89594
Waveguide parameters at wavelength [um]: 1.5265
Group index: 4.1648
Dispersion [ps/nm/km]: -251.0865

Simulated Data from Output Grating Coupler 2
Mean Group Index = 4.1842

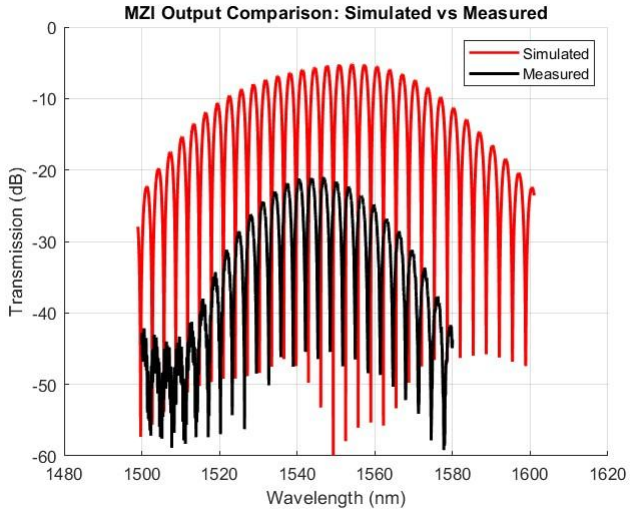

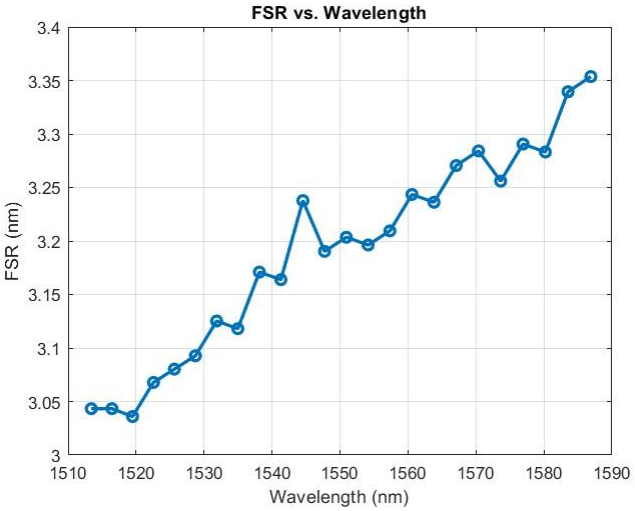

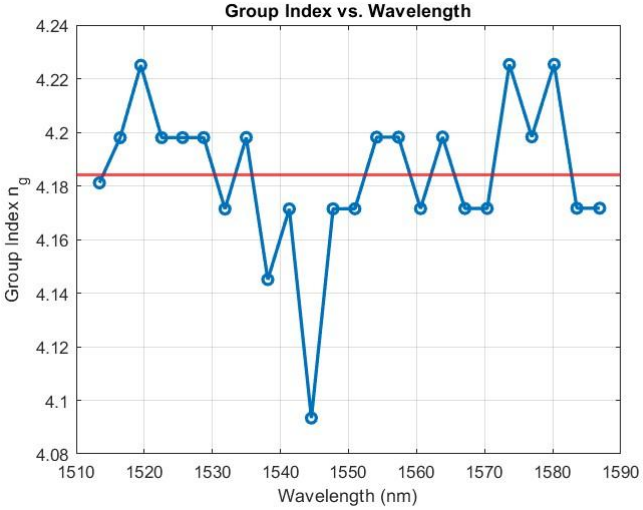

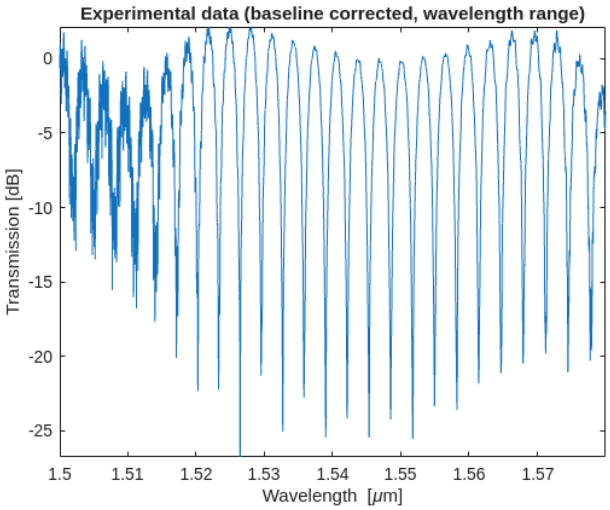

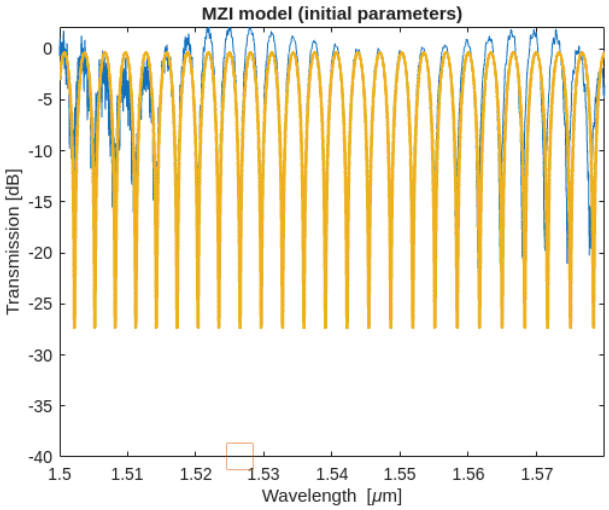

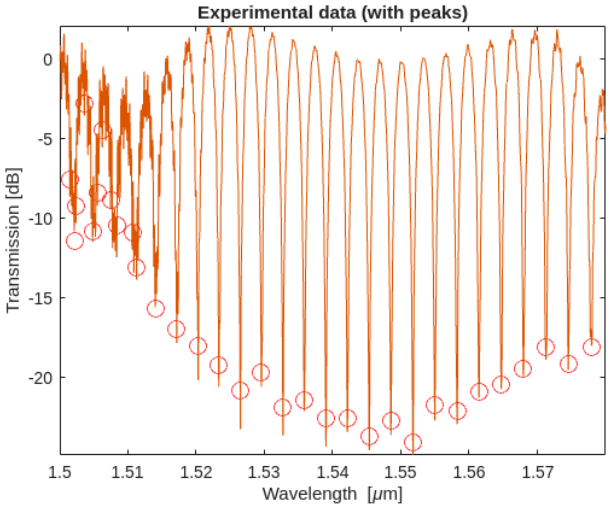

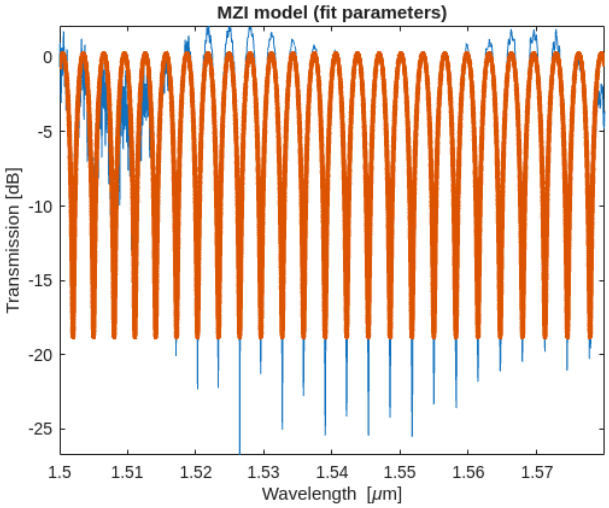

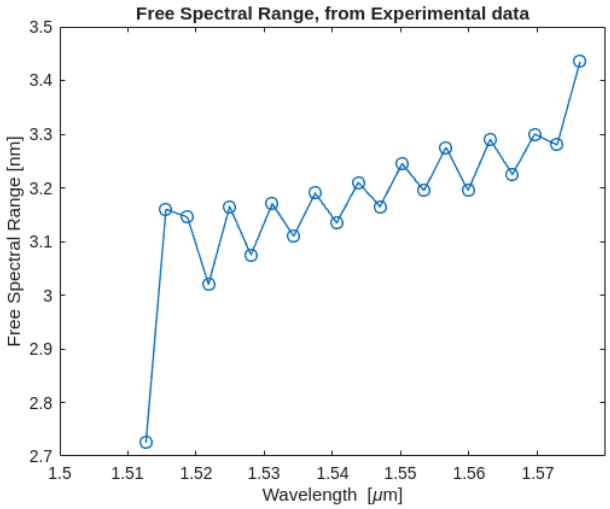

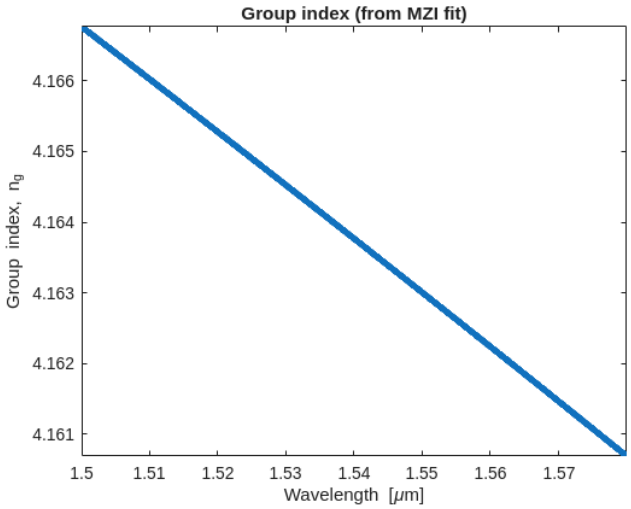

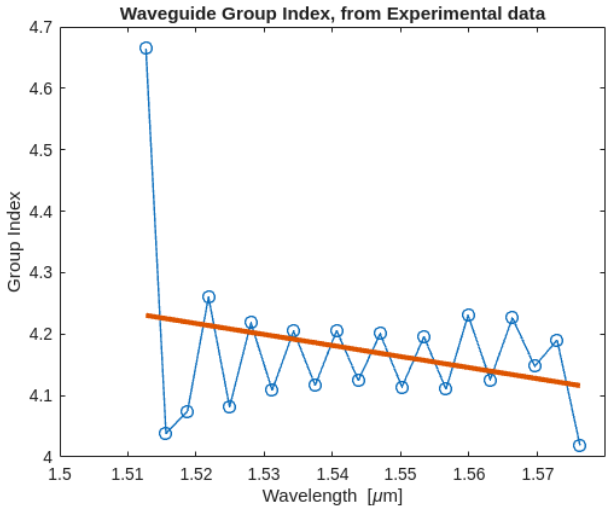

7. Conclusion

In this report, a basic study on the effect of path length differences in MZIs has been done and analyzed. Additionally, the mean group index and the free spectral range values at different wavelengths have been compared between the simulated data and the experimental data. The presence of these experimental group index values across the different MZIs within less than 1% (except in MZI3 where it is 4.97%) of the corresponding simulated values show the precision and scalability of silicon photonics fabrication techniques. The only significant difference is the much higher insertion loss in experimental data in comparison to the simulated data which is expected and can be attributed to the unavoidable prototyping imperfections, optical loss to materials, coupling loss and other surrounding factors.

Acknowledgements

I acknowledge the edX UBCx Phot1x Silicon Photonics Design, Fabrication and Data Analysis course, which is supported by the Natural Sciences and Engineering Research Council of Canada (NSERC) Silicon Electronic-Photonic Integrated Circuits (SiEPIC) Program. The devices were fabricated by Richard Bojko at the University of Washington Washington Nanofabrication Facility, part of the National Science Foundation's National Nanotechnology Infrastructure Network (NNIN), and Cameron Horvath at Applied Nanotools, Inc. Enxiao Luan performed the measurements at The University of British Columbia. I acknowledge Lumerical Solutions, Inc., MathWorks, Mentor Graphics, Python, and KLayout for the design software.

References

[1] Lukas Chrostowski, Michael Hochberg. Silicon Photonics Design. Cambridge University Press (CUP), 2015.
DOI: https://dx.doi.org/10.1017/cbo9781316084168

[2] Lukas Chrostowski, Michael Hochberg. Testing and packaging. 381–405 In Silicon Photonics Design. Cambridge University Press (CUP).
DOI: https://dx.doi.org/10.1017/cbo9781316084168.013

[3] Yun Wang, Xu Wang, Jonas Flueckiger, Han Yun, Wei Shi, Richard Bojko, Nicolas A. F. Jaeger, Lukas Chrostowski. Focusing sub-wavelength grating couplers with low back reflections for rapid prototyping of silicon photonic circuits. Opt. Express 22, 20652 The Optical Society, 2014.
DOI: https://dx.doi.org/10.1364/oe.22.020652

[4] Simulation and Design of Mach–Zehnder Interferometer. Priyanka Bhardwaj, Manidipa Roy & Sanjay Kumar Singh. Conference Paper. 2022.
DOI: http://dx.doi.org/10.1007/978-981-16-8721-1_47

[5] R. J. Bojko, J. Li, L. He, T. Baehr-Jones, M. Hochberg, and Y. Aida, "Electron beam lithography writing strategies for low loss, high confinement silicon optical waveguides," J. Vacuum Sci. Technol. B 29, 06F309 (2011)
DOI: https://doi.org/10.1116/1.3653266

[6] Lukas Chrostowski, Michael Hochberg, chapter 12 in "Silicon Photonics Design: From Devices to Systems", Cambridge University Press, 2015

[7] https://siepic.ubc.ca/probestation, using Python code developed by Michael Caverley.

[8] Yun Wang, Xu Wang, Jonas Flueckiger, Han Yun, Wei Shi, Richard Bojko, Nicolas A. F. Jaeger, Lukas Chrostowski, "Focusing sub-wavelength grating couplers with low back reflections for rapid prototyping of silicon photonic circuits", Optics Express Vol. 22, Issue 17, pp. 20652-20662 (2014)
DOI: https://dx.doi.org/10.1364/OE.22.020652

[9] https://www.plcconnections.com, PLC Connections, Columbus OH, USA.

[10] https://mapleleafphotonics.com, Maple Leaf Photonics, Seattle WA, USA.